NASA Contractor Report 4158

Design and Demonstration of a System for the Deposition of Atomic-Oxygen Durable Coatings for Reflective Solar Dynamic Power System Concentrators

Donald J. McClure

CONTRACT NAS3-25075
JULY 1988

NASA Contractor Report 4158

Design and Demonstration of a System for the Deposition of Atomic-Oxygen Durable Coatings for Reflective Solar Dynamic Power System Concentrators

Donald J. McClure
3M Corporation
St. Paul, Minnesota

Prepared for
Lewis Research Center
under Contract NAS3-25075

National Aeronautics
and Space Administration

**Scientific and Technical
Information Division**

1988

FOREWORD

This report summarizes the work accomplished under NASA Contract NAS3-25075, "Design and Demonstration of a System for the Deposition of Atomic-Oxygen Durable Coatings for Reflective and Refractive Solar Dynamic Power System Concentrators." The program was sponsored by NASA Lewis Research Center (LeRC). Daniel A. Gulino was the NASA Project Manager; Paul R. Johansen was the 3M Program Manager; Donald J. McClure was the 3M Principal Investigator. The Government Aerospace Systems Division of the Harris Corporation participated as a subcontractor to 3M; Donald E. Morel was the Harris Program Manager.

The program was divided into two tasks which addressed the following:

Task 1.0 Deposition System Design

Task 2.0 Coating System Performance Demonstration

The final subtask, Subtask 2.4, Coating of an Indefinite Number of Facets, had not started at the time this report was written.

This Page Intentionally Left Blank

TABLE OF CONTENTS

1 SUMMARY

The objectives of this program were to design and demonstrate a system for the vacuum deposition of atomic-oxygen durable coatings for reflective solar dynamic power system (SDPS) concentrators. The design issues pertinent to SDPS have been developed by the Government Aerospace Systems Division of the Harris Corporation and have been described previously.[1]

Both the design phase and the demonstration phase have been completed. At the time of this report the deposition system was ready for coating of facets for SDPS concentrators. The materials issues relevant to the coating work were not entirely resolved however. These issues can only be resolved when substrates which are comparable to those which will be used in flight hardware are available. The substrates available during the contract period were deficient in the areas of surface roughness and contamination. These issues are discussed more thoroughly in the body of the report.

2 INTRODUCTION

The overall objectives of this program were:

1. to provide NASA-LeRC with a detailed design for a vacuum thin film deposition system capable of depositing qualified atomic oxygen durable coatings for Solar Dynamic Power System (SDPS) reflector facets;

2. to demonstrate the capabilities of the system on full scale mock-ups of SDPS reflector facets; and

3. to coat an indefinite number of facets.

At the time of this report the third objective, the coating of facets, had not started. The design issues pertinent to SDPS have been developed by the Government Aerospace Systems Division of the Harris Corporation and are described elsewhere.[1]

This report describes the work carried out in satisfying the objectives supported by NASA-LeRC as well as the results of a parallel effort supported by 3M. The body of the report is organized to reflect the task structure set out in the contract with additions made to reflect changes and additions which were not in the original contract.

2.1 LEO durability

The deposition system developed as part of this program will be used to deposit reflective and protective coatings onto SDPS facets and mock-ups. The stated intent is to provide samples which are atomic-oxygen durable. In a larger sense, the intent is to coat facets and samples which are durable in low earth orbit (LEO). This section discusses some of the durability issues with respect to reflective and protective films both in atomic oxygen and in LEO.

The criterion of atomic-oxygen durability, rather than LEO durability, is readily understood in terms of the accessibility of atomic oxygen simulation tests compared to actual tests in LEO. The absence of a definitive and comprehensive model of materials degradation in LEO precludes designing, with complete assurance, a durable coating based on results from tests performed in other environments, which then require extrapolation to LEO conditions. Therefore the criterion used in this work was performance following exposure to atomic oxygen in a plasma asher or other oxygen plasma device.

The major components of the LEO environment pertinent to coatings durability are highlighted here. The dominant chemical constituent of the LEO environment is atomic oxygen; its erosive potential is substantially enhanced by the high speeds of the

Space Station (SS) on orbit. Solar radiation in the UV-VIS-IR region is intense and may impact materials durability in LEO. The SDPS facets will be subject to substantial temperature variations as the Space Station moves from full sun to eclipse. Micrometeoroids are expected to affect the durability of coatings. A more detailed discussion of these components is presented below.

2.1.1 Atomic Oxygen

The Space Station will operate in a nominal orbit between 200 and 250 nautical miles which corresponds to low or near earth orbit. Early STS missions recorded evidence of thermal blanket degradation (mass loss and changes in front surface optical properties) which was attributed to atomic oxygen effects. Atomic oxygen is the dominant chemical constituent found at the operational altitudes proposed for the Space Station, as indicated in Figure 2-1. The number density of oxygen atoms is of order 10^9 atoms/cm^3, corresponding to a pressure of about 10^{-6} Pa (10^{-8} Torr). However the high velocity of the orbiting SS (about 8 km/sec) results in a flux of about 10^{15} atoms/cm^2-sec. This flux is equivalent to that observed at a stationary surface at a pressure 300 times higher than the nominal value. Moreover the velocity of the SS relative to the oxygen atoms results in an energy of bombardment of nearly $8x10^{-19}$ joules/atom (4 eV/atom). Figure 2-2 illustrates the density and flux of atomic oxygen as a function of altitude (assuming a nominal velocity of 8 km/sec).

The overall effects of atomic oxygen ram impacts will be a function of orbital altitude and inclination, solar activity, spacecraft geometry, mission lifetime, and impingement flux and angle. Materials with high reaction efficiencies will need to be protected in order to prevent loss of mass and front surface optical properties. This will be especially critical for the solar concentrator: loss of front surface optical properties will directly impact the power system efficiency.

Some of the degradation which has been observed on surfaces exposed to this flux can readily be explained in terms of the effects of atomic oxygen. For example, silver will oxidize on exposure to atomic oxygen and to ozone, as well. Therefore the oxidation of silver observed in the shuttle environment is not surprising. The protective coatings to be delivered as part of this program must protect sensitive surfaces against atomic oxygen.

Coatings to protect sensitive surfaces must not only be resistant but must also completely cover the sensitive surfaces with no pinholes or other defects. A common long term failure mode for sensitive coatings used in terrestrial environments is the growth of a defect area through a pinhole in the protective overcoat. Frequently the area effected is large compared to the size of the pinhole. Lateral diffusion of erosion reactants and products can

lead to a substantial loss of functional performance on an area basis. The coatings developed in this program were not specifically evaluated for pinhole densities or the consequences of pinholes. The durability demonstrated for these coatings in atomic asher testing suggests however that pinholes are not a problem in the time domain sampled by the tests.

Other observations suggest that the presence of atomic oxygen is not sufficient to explain all of the degradation observed. The rapid weight loss of polyimide films (Kapton) on orbit is an excellent example. Several terrestrial experiments indicate that polyimide is ablated at very low rates by atomic oxygen at thermal energies in its ground electronic state. When atomic oxygen is accelerated (to 0.14 ev) using nozzle beam techniques Kapton surfaces are ablated albeit at lower rates than on orbit. This suggests that the Kapton erosion on orbit is due in part to the high translation energies of the impinging atoms. It may also be related to the large fluxes of UV radiation in concert with the energetic atoms. This effect could occur through activation of the surface by UV photons followed by reaction with oxygen and subsequent desorption, for example. The graphite-epoxy substrate for the facets coated under this program will require protection on their edges and back surfaces.

2.1.2 Radiation

The solar irradiance at air mass zero is shown in Figure 2-3. The peak irradiance occurs in the visible near 500 nm (2.5 eV) but significant flux occurs at shorter wavelengths (higher energies) extending to slightly below 200 nm (6 eV). Surfaces proposed for exposure on SS must be durable with respect to this radiation as well.

In the specific application of interest silver is the reflective material of choice. Silver has a window near 320 nm (3.9 eV/ photon) in which large fractions of the incident radiation is transmitted. If the silver film were coated onto a graphite/epoxy composite substrate, some radiation at that energy would be transmitted. While bulk changes in the epoxy are not anticipated, normally small changes which occur at the interface between the epoxy and a thin silver film could produce significant deterioration of the epoxy/silver system performance. A small bubble might lead to a pinhole, which in turn could lead to erosion of the silver and loss of optical performance.

2.1.3 Temperature fluctuations

The coatings to be prepared will ultimately have to withstand significant temperature variations due to alternate periods of full solar irradiation and eclipse. Care was used in the materials selection process to avoid materials which would lead to fracture of the films due to thermal cycling.

2.1.4 Micrometeoroids

In order to withstand the impact of micrometeoroids, the film-substrate composites should be developed with sensitivity to their brittle behavior. Ultimately a self-healing coating would be desirable but is beyond the scope of the current effort.

2.1.5 Summary

We have presented a brief overview of our understanding of the LEO environment related to the durability of reflective and protective coatings. This material bears directly on the long range goals of the program even though atomic oxygen (not LEO) durability is stated objective. This material is particularly relevant as the SDPS program develops and requires LEO qualified facets with durabilities which permit nominal operation for a seven to ten year period.

We conclude this section with a brief summary of the energies relevant to LEO. Atomic oxygen is a reactive free radical which can be formed from molecular oxygen by the addition of about 2.6 eV per atom. The translational energy of atomic oxygen at SS flight altitudes is about 4 eV. The energies of the solar radiation extend at high intensities up to 5 or 6 eV. Bond energies for polymeric materials are of order 3.5-4 eV (single bonds).

3 TECHNICAL APPROACH/RESULTS

3.1 Task 1.0 Deposition System Design

The objective of Task 1.0 was to develop the design of the vacuum deposition system to coat atomic oxygen durable coatings onto SDPS facets. The design was based on inputs from NASA and from knowledge of the contract team.

3.1.1 Subtask 1.1 Technical Briefing/Design Specification

The objective of Subtask 1.1 was the transfer of the latest information relevant to the Design Specification from NASA to the contract team. Some of the materials information had been previously published.[2] New information on the durability of coated and uncoated aluminum films was also presented. As noted below in Section 3.1.7.1 that material was judged to be of little value to this program and hence is not given here. Also new information on the response of protected reflectors to plasma asher exposure following damage by particle impacts was presented. The details of that work have now been reported.[3] The NASA decision in favor of a reflective, rather than refractive, concentrator concept was formally presented.

3.1.2 Subtask 1.2 Prepare/Present Design Concept

The objectives of Subtask 1.2 were to develop specific recommendations for a substrate material, facet geometry, reflective material, protective material, coating thickness, and method of deposition for atomic oxygen durable coatings and to prepare a preliminary design concept for a deposition system capable of satisfying those criteria. The recommendations made as part of this subtask are presented in this section

3.1.2.1 Facet geometry

The facet geometry is taken from the deployable truss hex design in the offset configuration as selected by NASA based on the SCAD study at Harris.[1] The facets are equilateral triangles, one meter on a side, with spherical radii for different facets ranging from 19-30m.

3.1.2.2 Substrate material

The substrate material is a critical element in virtually all thin film coated products. The material chosen, again based of the SCAD study[1] was graphite-epoxy facesheets bonded to a vented, aluminum honeycomb core. The range of graphite-epoxy materials which had been investigated by Harris have been described.[1] It was noted at the time of this selection that work was underway to develop processes to manufacture facets with appropriate surface quality in terms of surface smoothness and freedom from defects.

The facet manufacturing process and the final substrate material selection are part of other contract work. At the time of this report the details of the process and the materials to be used were not fully resolved. Figure 3-1 is a diagram of the facet selected.

3.1.2.3 Method of deposition

The method of deposition recommended and used employed an electron-beam evaporation source. Such sources are quite versatile, and the one chosen for use permitted up to four different coating materials to be deposited in any order without exposure of the facet to the atmosphere. The deposition system also had a glow discharge electrode which has been used to pretreat the graphite-epoxy substrates for improved adhesion.

3.1.2.4 Preliminary design

The preliminary design proposed and implemented involved modifying a commercially available deposition system, a Denton Model DVB-44, to suit the requirements of this project. Uniformity of coating thickness would be achieved by rotation of a tilted facet during coating, with the source offset from the facet center line to give a calculated thickness uniformity of 6%, that is, the thinnest areas would be 6% thinner than the thickest areas. The uniformity specifications in the RFP were defined as no more than 5% variation in the thickness over the surface area of the facet. The NASA Project Manager agreed that deviation greater than 5% would be acceptable. The basis for the thickness uniformity projection is given below.

3.1.2.5 Thickness uniformity

The thickness uniformity profiles of films formed by evaporation from small area sources often behave like $\cos^4 \theta$, where θ is the angle between the line drawn between the source and a point on the substrate surface and the normal to the substrate. This geometry is shown schematically in Figure 3-2a; the resultant thickness uniformity distribution is shown in Figure 3-3a. This distribution is clearly inadequate for the requirements of this program.

The $\cos^4 \theta$ dependence arises from three effects. Typical small area sources have a $\cos \theta$ dependence of their flux distributions measured on a spherical surface centered at the evaporation source. A factor of $\cos^2 \theta$ arises from the r^{-2} dependence of the flux with distance, r, from the source. The last $\cos \theta$ factor is due to the angle of the substrate surface to the direction of the incident flux away from the source center line. Note that the radius of curvature of the most curved reflector facet is of order 18m. This value was judged large enough to permit neglecting the effect of surface curvature in the calculation.

By rotation of the facet on its own center and placing the source near the edge of the circumscribed circle, one obtains a thickness uniformity profile which is very approximately $\cos^2 \theta$, where θ is now the angle between a point on the substrate surface and the point on the axis of rotation of the substrate at a distance from the substrate equal to the throw distance. This geometry is shown schematically in Figure 3-2b; the resultant thickness uniformity distribution is shown in Figure 3-3b. Finally if the axis of rotation of the substrate is tilted to reduce the source-substrate distance immediately over the source as shown in Figure 3-2c, thickness uniformities of better than 6% can be achieved, as shown in Figure 3-3c.

As noted below in Section 3.1.5.1, the source distribution was measured and was well approximated by a $\cos^2 \theta$ rather than $\cos \theta$. The final design was modified to accommodate this effect.

3.1.2.6 Reflectance uniformity

The uniformity of reflectance was not calculated. Rather we proposed to proceed on a best efforts basis. Our expectations that the reflectivity would be uniformly high were realized as discussed in Section 3.2.3.4.

3.1.2.7 Reflective material

Reflective concentrators for SDPS require high levels of solar specular reflectance. The materials considered in the proposal stage included silver (Ag), aluminum (Al), platinum (Pt), rhodium (Rh), and iridium (Ir). Reflectivity data for these five metals are plotted in Figure 3-4. It is clear from the data in Figure 3-4 that Al and Ag have the highest reflectivities. Integrating the product of the reflectivities and the relative solar spectral irradiance produces a figure of merit (the solar spectral reflectance) for the relative performance of the candidate metals. The results are shown in Table 3-1. The calculations used a moderately coarse, piece-wise continuous approximation to the solar spectral irradiance and neglected contributions from wavelengths greater than 3 microns. The results are thus indicative rather than definitive. They are normalized to an ideal reflector which would have a figure of merit of unity.

Table 3-1. Figures of merit for reflectivity

Metal	Solar spectral reflectance
Ag	0.92
Al	0.93
Rh	0.81
Ir	0.74
Pt	0.68

As suggested by observation, Ag and Al yield higher average reflectivities with the remaining metals significantly lower. In so far as the curves represent the performance of films suitable for SDPS, Al and Ag are the best choices for SDPS reflector surfaces, provided that they can be delivered in atomic oxygen durable constructions.

Al has significant advantages over Ag for terrestrial based mock-ups in terms of atmospheric corrosion resistance, due largely to the formation of a protective, native oxide on Al. The susceptibility of unprotected Ag to damage from atomic oxygen in LEO is also significant. Finally the drop in reflectivity of Ag at about 320 nm corresponds to a region where Ag transmits light. This feature may have a deleterious effect on a graphite-epoxy substrate/Ag film reflector composite.

Rh is in third position in Table 3-1. It is widely used as a reflector in a variety of optical systems because it is a hard, durable, noble metal that is resistant to chemical attack. Its resistance to salt spray, for example, often makes it the reflective metal of choice. Because effective protective overcoats were demonstrated for Al and Ag, no work on Rh was performed.

3.1.2.8 Protective material

The protective material plays a crucial role in the long-term performance of SDPS. The initial performance of the system will largely be defined by the substrate and reflector characteristics, although the reflectivity of Al can be seriously degraded by overcoating (see Section 3.1.7.1). Maintenance of the initial performance level with minimum degradation over its operational life will clearly depend on the protective material.

The candidate protective materials were aluminum oxide (Al_2O_3), silicon dioxide (SiO_2), and magnesium fluoride (MgF_2). A large number of reflective/protective layer combinations have been evaluated with emphasis on Al and Ag reflective layers. The results of that work have been published.[1] In summary Ag yields higher integrated reflectances than Al, and several protective

coatings exhibit excellent resistance to atomic oxygen degradation for both reflective coatings. Sample curves for Ag and Al surfaces protected with various protective coatings showing total and specular reflectivity as a function of atomic oxygen exposure time have also been published.[1]

3.1.2.9 Coating thickness

The reflective layer coating thickness does not now seem to be crucial to the performance of the SPDS. Clearly coatings which are too thin (less than a few tens of nm) may reduce the spectral reflectivity, and coatings which are too thick (greater than a few hundred nm) may begin to suffer from intrinsic stress problems. Al films often exhibit decreased reflectance as the thickness exceeds a few hundred nm due to formation of large grains in the films which result in a faceted surface which in turn scatters light. Such films have a matte appearance. Coatings of intermediate thickness (of order 50-100 nm) are expected to be satisfactory. The protective layer coating thickness can affect the optical performance of Al reflectors significantly (see Section 3.1.7.1) but has little effect on Ag reflectors. Again too thin a coating may not afford protection and too thick may lead to stress problems.

3.1.2.10 Reflective material, protective material, coating thickness

The candidate materials evaluated as described in Sections 3.1.2.7 and 3.1.2.8 were deposited by a variety of methods, but not by electron-beam evaporation as was proposed here. Moreover important parameters such as protective layer thickness were not readily available. Good performance by these materials demonstrates the existence of durable coating combinations, but bad performance only indicates that the particular sample failed. It was therefore proposed and approved that 3M would evaluate electron-beam deposited materials (Ag and Al reflector layers with SiO_2, Al_2O_3, and MgF_2 protective layers) and would evaluate all materials for atomic oxygen durability and high specularity into narrow angles more appropriate for SDPS. This effort would allow materials selection to be made on the basis of evaluations of coatings prepared using the processes proposed for the actual facets.

It was agreed that this work would be carried out at 3M's expense in parallel to the efforts in Subtasks 1.3-1.5 and targeted for completion at the time of completion of Subtask 1.4 and 1.5.

3.1.2.11 Substrate surface roughness

The roughness of the graphite-epoxy substrate surfaces was cause for concern for two reasons. First, the roughness would cause a loss in specular reflectance from what might be obtainable from

better surfaces and hence lead to a reduction in system efficiency. This effect had been recognized but not addressed systematically; it was addressed as part of Subtask 1.2. A summary is given below. Second, roughness features with steep side walls would reduce the local thickness of the deposited thin films. The thickness reduction could cause a decrease in the durability of the protective coatings and hence lead to a reduction in the lifetime of thin film reflective coating performance. This effect can only be addressed when substrates which are characteristic of those which will be used in flight hardware are available and may affect the ultimate materials selection.

The effects of surface roughness on specular reflectivity have been treated in a paper by H. E. Bennett and J. M. Bennett.[4] The authors distinguish between three ranges of surface roughness, depending on the size of the surface features relative to the wavelength of light.

In the first range, the roughness features are much larger than the wavelength of light and therefore geometrical optics apply. They note that often for surfaces of this type the measured total reflectance is smaller than that of a perfectly smooth surface of the same material due to trapping of the light in the surface facets. The low values for total reflectance obtained for some coated graphite-epoxy composite surfaces reported in Reference 1 may be understood in that context.

In the second range the roughness is comparable to the wavelength, and diffraction effects become important. However the modeling is difficult.

Finally in the third range, the roughness is smaller than the wavelength, and the modeling is simplified. In this range the reflectivity expressed as the ratio of the observed reflectivity, R, divided by the reflectivity of a perfectly smooth surface of the same material, Ro, is given as:

$$R/Ro = \exp(-(4\pi\sigma\cos\theta/w)^2) + \text{incoherent term},$$

where σ is the rms surface roughness,
θ is the angle of incidence,
and w is the wavelength.

The model assumes Gaussian surface roughness, usually a good assumption (see below). The incoherent term is treated in some depth in the original paper, but the authors remark that "if R/Ro>0.9, the incoherent term may usually be assumed to be negligible for an instrument acceptance angle of 0.03 sr or smaller." Since 0.03 sr solid angle is equivalent to 175 mrad, SDPS models should be able to neglect the incoherent term.

It is appropriate to note that an alternative description to the one given above has been presented by R. B. Pettit and E. P. Roth.[5] The work described here was performed before that reference was obtained and does not incorporate their ideas. The following remarks are therefore given as a record of the work performed but may be superceded by a more complete and appropriate description in the future.

As a rough approximation, the Gaussian was expanded keeping the term in $(\sigma/w)^2$ and neglecting higher terms. For simplicity non-normal incidence was neglected. Therefore:

$$R/Ro = 1 - (4\pi\sigma/w)^2$$

H. E. Bennett and J. L. Stanford have published[6] the results of calculations which predict the scattering as a fraction of the light lost as a function of roughness and wavelength. Their Figure 4 plots lines of equal loss on a plot of wavelength and roughness and identifies a metal surface with a normal polish with a roughness of 6 nm. Note that "normal" in this regard is normal for optical science on flat surfaces over a few centimeters but not for conventional fabricated surfaces (facets) which are neither small nor flat. As read from the figure, the normal polished metal surface is projected to lose 1% at 750 nm increasing to 10% at 240 nm. Rougher surfaces would of course produce greater losses.

It is appropriate to ask whether the results of the theory are borne out in observations. L. J. Cunningham and A. J. Braundmeier, Jr.[7] have published measured reflectance versus wavelength for silver films with different surface roughnesses. Their Figure 1 gives results for three films. The roughest had a surface roughness estimated to be 2.6-3.1 nm rms and showed a reflectivity of ≈73% at 400 nm and ≈82% at 500nm. These values are much lower than the comparable values for their smoothest film which were 95% and 97%, respectively. Note that the reflectance losses are much larger than the theory would predict. This can be understood in two ways. First the roughness of their surfaces might not have been Gaussian. In fact the authors give reason to believe that they were not. Second the spectra are given very near to the surface plasmon region in silver, and so the losses are aggravated by that effect. H. E. Bennett and J. L. Stanford[8] note that surface plasmon effects in Al are important over a much broader range than in Ag. They did not indicate what the magnitude of the effect would be, however. Note that both Ag and Al will be subject to such plasmon enhanced losses. When the actual substrate surface used is better defined, the magnitude of the losses will need to be considered in choosing the reflector material.

If the losses due to surface plasmon interactions are ignored, an appraisal of the impact of this reflectance loss on SDPS can be

made. Clearly the assumptions on which the model is based limit its applicability. However H. E. Bennett and J. M. Bennett,[9] have shown that, for some surfaces at least, the measured reflectance follows the Gaussian model to well beyond the range where the model can be proven to apply. The words "some surfaces" needs to be emphasized: this may not apply to all surfaces.

The calculations cited above generate losses as a function of σ/w. For the specific case of SDPS, an average over the solar spectrum as a function of σ is needed. The model developed here truncates the expansion of the Gaussian at the quadratic term in σ/w and averages over the AM0 spectrum. The results are shown in Figure 3-5, and indicate the loss (in this approximation) one would expect in the reflectance due to surface roughness from an otherwise perfect reflector. Note that a surface with a Gaussian surface roughness of 6 nm (a metal with a "normal polish") produces a loss of almost 2% due to roughness alone. The losses increase rapidly for rougher surfaces. This model has many shortcomings but does suggest a more thorough appraisal of these effects be made.

3.1.3 Subtask 1.3 Prepare/Present Preliminary Design

The preliminary design was presented and approved.

3.1.4 Subtask 1.4 Prepare/Present Final Design
3.1.5 Subtask 1.5 Prepare/Present Fabrication Plan

The final design and fabrication plan were approved with some discussion of details of the design. Errors in the drawings were corrected, and six complete sets of drawings with errors corrected were delivered to NASA-LeRC. During this contract period the NASA Project Manager requested that project work be accelerated so as to be ready for Subtask 2.4 by July, 1987, reducing the project duration by 2.5 months. This request was accommodated.

3.1.5.1 Coating thickness uniformity

The position of the source within the coater and the angle of inclination of the facet during coating both affect the coating thickness uniformity. Both of those parameters were fixed as part of the final design. The following section described the results of measurements taken and calculations performed which lead to the values selected.

In order to effectively model the coating thickness uniformity it was necessary to determine the actual thickness distribution from the electron-beam source. To that end measurements of the coating thickness on stationary substrates as a function of position within the coating chamber were made for aluminum and silicon dioxide coatings. Aluminum and silicon dioxide were used as prototypes of the reflective and protective layers.

The results of the thickness uniformity measurements are described below. Figure 3-6 shows the predicted relative thickness values for stationary substrates as a function of position in the coater assuming three different source flux distributions, modeled as the first, second, and third power of the cosine of the angle away from the vertical. The position corresponding to 0 was the wall of the coater. This plot was generated to indicate the sensitivity of the result to the source model used. Figures 3-7 and 3-8 show the measured results for SiO2 and Al, respectively. Both are well fit by a cosine squared source flux distribution at positions greater than 30 cm. The divergence of the Al data at positions less than 30 cm has not been explained.
This data was the used to position the source within the coater for optimum thickness uniformity. Using that position, the thickness uniformity for coating onto rotating facets was calculated. The results are shown in Figure 3-9 with the angle of inclination as a parameter. The data in Figure 3-9 suggest that the optimum angle is 20-21° and that the thinnest area on the substrate will be slightly more than 91% as thick as the thickest area. The thickness uniformity measured as part of Subtask 2.3 is very close to that predicted here.

3.1.6 Subtask 1.6 Consultation

This Subtask was not exercised as the Final Design and the Fabrication Plan were approved without need for this consultation.

3.1.7 3M Sponsored Materials Effort

The results of a 3M sponsored materials effort first described in Section 3.1.2.10. are presented below. The effort divides into three subsections: optical modeling, materials preparation and results, and materials selection.

3.1.7.1 Optical Modeling

Optical modeling was performed to estimate the effects of the protective layer thickness on the reflectivity. Specifically the reflectivity as a function of wavelength was calculated for several combinations of reflector metal and protective layer materials. Figures 3-10, 3-11, and 3-12 show the results for Ag with SiO_2, Al with SiO_2 (index = 1.46), and Al with Al_2O_3 (index = 1.63), respectively. Clearly the reflectivity of Al is affected more by overcoating than that of Ag. Also the reflectivity of Al is affected more by overcoats having a higher index. Figure 3-13 shows the results for a series of dual layer protective coatings on Ag consisting of 20 nm of Al_2O_3 with various thicknesses of SiO_2 overcoats. Figure 3-14 shows the effects of incidence angle on the reflectivity, which is small for Al and smaller still for Ag (not shown).

The plots of the reflectivity as a function of wavelength are valuable in understanding the trends, but the more relevant information is the calculated reflectance spectra convoluted with the AM0 spectrum to give integrated reflectance as a function of overcoat thickness.

Figures 3-15 and 3-16 show the results of convolution of a number of calculated spectra with the AM0 spectrum to give relative specular solar reflectivities. These values were then plotted against the protective overlayer thickness for SiO_2 on Ag and Al, Figure 3-15, and Al_2O_3 on Ag and Al, Figure 3-16. Figure 3-17 is the same as Figure 3-15 except calculated for a 45 degree angle of incidence.

It becomes clear from the results of these calculations that Al reflectors are far more sensitive to the effects of overcoating than Ag ones. Many of the reflector samples prepared prior to this effort and early in this effort were overcoated with dielectrics whose target thicknesses were close to 100 nm. The results shown in Figures 3-15 and 3-17 suggest that the wide variability in the measured reflectivities can now be understood in terms of optical effects. The protective layer thicknesses chosen were arguably the worst possible thicknesses for use with Al reflectors. The sensitivity of the reflectivity of Al coatings to the thickness of overcoats in this thickness domain makes evaluation of much of the Al data described in Sections 3.1.1 and 3.1.2.10 difficult without detailed knowledge of the optical thickness (thickness and index) of the overcoats.

Figure 3-18 is a measured spectrum of a protected Ag film presented to show an actual value of the transmission feature near 320 nm. There is some concern that this transmitted light could adversely affect the stability of the epoxy composite substrate. We are unaware of any data which can be used to estimate what effect this exposure would have on the epoxy.

3.1.7.2 Materials Preparation and Results

The materials preparation effort was carried out to evaluate the performance of reflective and protective films prepared by electron-beam evaporation, the process to be used in production of coated facets. The emphasis was on preparation of films combinations which were durable under oxygen asher exposure and had high specular reflectivity.

The reflectivities were measured using a Perkin-Elmer Lambda 9 UV-VIS-NIR spectrophotometer equipped with a 60 mm integrating sphere. The oxygen plasma exposure was carried out in a Perkin-Elmer Randex 2400-8SA rf sputtering system. The samples were suspended vertically from the edge of the horizontal shutter assembly, not on the substrate table. Oxygen was admitted at 80 sccm, and the throttle valve over the diffusion pump was adjusted

so as to maintain a pressure of 20 mTorr. A plasma was generated by capacitively coupling 200W of 13.56 MHz excitation to the system substrate table. The erosion rate for Kapton under these conditions was measured gravimetrically to be 0.4μm/hour.

The coatings combinations prepared in the first set of samples were:

Al (70nm)
Al (70nm), Al_2O_3 (100 nm)
Al (70nm), SiO_2 (100 nm)
Al_2O_3 (10 nm), Ag (70 nm), Al_2O_3 (100 nm)
Al_2O_3 (10 nm), Ag (70 nm), Al_2O_3 (30 nm), SiO_2 (70 nm)

The substrates were silicon, quartz, and graphite-epoxy. The silicon and quartz substrates were used to provide smooth surfaces for reflectance measurements; the graphite-epoxy was used to evaluate durability of the coating combinations on the material which would ultimately form SDPS facets. The first three sample sets were prepared in an effort to compare bare Al with Al coated with Al_2O_3 and SiO_2. The later two sets used Al_2O_3 as an adhesion promotion layer on either side of the Ag. It has been reported that Al_2O_3 does not form an effective barrier to moisture penetration and so the last sample was prepared with a dual protective layer of Al_2O_3 and SiO_2. The thicknesses were chosen intuitively. Optimization of layer thicknesses was planned as a second phase of the effort.

The specular reflectance of the samples as a function of oxygen plasma exposure time are shown in Figures 3-19 to 3-20. All the samples on graphite-epoxy substrates cracked after between 72 and 132 hours of exposure. The parallel set tested at NASA-LeRC cracked after less than 52 hours. It should be noted that the substrate material used was not optimized and excellent performance has been observed in the past and more recently from coatings on other (smoother) graphite-epoxy substrates. The data on the Al samples are adversely affected by the thickness of the overcoat (as noted above): higher reflectivities are projected for optimized thicknesses. However the Ag films showed the best reflectivities and have held up well. The samples tested at NASA-LeRC have been tested for much longer periods of time. The data generated by atomic oxygen exposure and reflectance measurements at 3M and NASA-LeRC were found to be comparable.

A second set of materials were prepared and are listed below.

Al_2O_3 (10 nm), Ag (70 nm), SiO_2 (30 nm)
Al_2O_3 (10 nm), Ag (70 nm), SiO_2 (50 nm)
Al_2O_3 (10 nm), Ag (70 nm), SiO_2 (200 nm)
Ag (70 nm), SiO_2 (200 nm)
Al_2O_3 (10 nm), Ag (70 nm), MgF_2 (200 nm)

The first three were an effort to optimize the protective layer thickness. The fourth was to assess the importance of the Al_2O_3 adhesion promotion layer. All of these samples failed after short duration exposures to the oxygen plasma, apparently due to the

lack of Al_2O_3 over the Ag. The fifth sample was a test of MgF_2 protective coatings. MgF_2 is soft unless deposited onto a heated substrate. Samples prepared as shown were readily scratched using gentle pressure with a solvent wet cotton swab. In contrast there was no visible damage to the Ag samples overcoated with either Al_2O_3 or Al_2O_3/SiO_2 in the previous sample set as a result of scrubbing with a solvent wet cotton swab.

3.1.7.3 Materials Selection

The Ag coated samples show high integrated reflectivity and have shown good durability during asher exposure when coated onto quartz substrates. The Al samples have lower integrated reflectivities and are also durable. The proclivity of Al films to convert to Al_2O_3 (not demonstrated in this work) and the modeling calculations which indicate substantial loss in reflectivity due to overcoats on Al make Al less desirable than a durable Ag reflector. No samples prepared on graphite-epoxy during this subtask survived asher exposure: therefore no conclusions could be drawn from the AO durability testing which were relevant to the choice of reflector. See Section 3.2.3.5 for results on graphite epoxy samples which did survive asher exposure. On the basis of these observations Ag was chosen as the reflective material with the caveat that durable Ag coatings on graphite-epoxy must be demonstrated before flight-ready facets hardware are produced.

Ag does not adhere well to graphite-epoxy. Our work showed good adhesion for graphite-epoxy/Al_2O_3/Ag samples. Adhesion was tested using tape peel tests with Scotch Brand Magic Mending Tape.

The protective layer chosen consisted of a dual layer of Al_2O_3 and SiO_2. SiO_2 would provide protection from atomic oxygen and moisture but did not adhere well to the Ag layers. Al_2O_3 adheres well and should be atomic oxygen durable but does not protect from moisture. The dual layer structure adheres well and provides protection from both atomic oxygen and moisture.

The individual film thicknesses were not optimized during this effort. The thicknesses selected were based on those used for the samples which demonstrated good performance in the first set of samples. Later work showed that the performance, as measured by reflectivity and atomic oxygen durability screening tests on the proposed materials combination, was not sensitive to film thickness over reasonable ranges (see Section 3.2.3). The effects of changing the film thicknesses on constructions which show good reflectivity and good oxygen plasma durability will only be able to be tested by long term exposure in an atomic oxygen environment with a large number of samples to eliminate errors due to random defects. This level of effort was beyond the scope of the current program and would probably be appropriate when the final materials definition is made.

As a result of these evaluations the following materials were selected under the extension of Subtask 1.2:

graphite-epoxy	substrate
Al2O3 (20 nm)	adhesion promoter
Ag (70 nm)	reflector
Al2O3 (20 nm)	adhesion promoter
SiO2 (70 nm)	protective layer

The adhesion promotor was changed later in this program. A detailed discussion of that issue can be found in Section 3.2.3.5.

3.2 Task 2.0 Coating System Performance Demonstration

The objectives of Task 2.0 included modification of the deposition system to satisfy NASA requirements, and the check-out, calibration, and demonstration of the system. The results of that effort are reported below. The last objective, the coating of an indefinite number of facets, was an option not yet exercised by NASA.

3.2.1 Subtask 2.1 Fabrication of Deposition System

The deposition system modifications were fabricated and installed without incident.

3.2.2 Subtask 2.2 Deposition System Check-out and Calibration

The deposition system check-out and calibration were performed in two phases. The first phase which involved defining the details of the electron beam evaporation process (evaporation rate, beam sweep rates and focussing, preliminary thickness calibration for Al_2O_3, SiO_2 and Ag) was carried out as part of the 3M supported materials characterization effort and earlier unrelated experience with the coating system. The second phase, supported by NASA, involved deposition runs using the new geometry installed as part of Subtask 2.1 to determine thickness uniformity and the absolute thickness calibration. That work is described here.

A facet mock-up made from sheet aluminum was installed in the coater. The facet inclination angle was set at 20.5° as suggested by the thickness uniformity calculations described in Section 3.1.5.1. Four small substrates were positioned on the facet, a deposition of SiO_2 was made, and the thicknesses were measured. The results, with measured thickness plotted versus position on the facet, are shown in Figure 3-21. These results suggested that the coating was relatively thicker at the center and thinner at the edge than predicted. Better uniformity would therefore result from moving the facet to higher angles. The angle was therefore set to 23°, the maximum angle mechanically accessible in the design. A second set of samples were coated and measured. As discussed in Section 3.2.3, this change was not required.

The absolute thickness measured for these samples allowed the tooling factor, a geometric correction factor, to be determined. The tooling factor is independent of material, and hence no metal depositions were needed as part of the calibration effort.

3.2.3 Subtask 2.3 Demonstration of Coating System Performance

The coating system performance demonstration was carried out in the presence of the NASA Project Manager, D. A. Gulino, on June 25, 1987. Three nominally identical deposition runs were performed with 50 quartz substrates (coupons) attached in predetermined positions on the facet mock-up for each run. The coupons were attached to the facet mock-up with double sided adhesive tape allowing the entire front face of each coupon to be coated. The full four layer coating described in Section 3.1.7.3 was deposited during each of the three runs. The position of the 50 coupons on the facet mock-up is shown in Figure 3-22.

As agreed before hand, a small number of coupons were retained by 3M for analysis of thickness and reflectance uniformity and repeatability. The coupons selected were coupons 1-20 in Run 1 and coupons 1, 5, 10, 15, and 20 in Runs 2 and 3. The coupons from Run 1 were used for demonstration of uniformity; the coupons from Runs 2 and 3 in combination with the comparable coupons from Run 1 were used for demonstration of repeatability. The remaining 120 coupons were hand carried to NASA LeRC by D. A. Gulino. The 30 coupons were delivered to NASA-LeRC at the end of the project.

The film thickness uniformity was measured using three techniques: x-ray fluorescence, profilometry, and ellipsometry. The x-ray fluorescence measurements were made on the 30 coupons retained by 3M. The profilometry and ellipsometry measurements were made on samples prepared later. The use of the full four layer coating in combination with no masking on the coupon surface precluded use of the latter techniques on the actual coupons. These points were noted early in the program, and it was agreed that the techniques described here (separate runs for ellipsometry and profilometry) would be appropriate.

3.2.3.1 Thickness determination using x-ray fluorescence

The x-ray fluorescence determination used a Rigaku Model 3370 wavelength dispersive x-ray fluorescence spectrometer. Relative silver thickness was determined using the Ag Kα line at 22.16 keV. Relative aluminum oxide thickness was determined using the Al Kα line at 1.49 keV. Because of its low energy the latter line may be attenuated somewhat by the SiO_2 overcoat. The Al intensities are proportional to the Al_2O_3 thickness provided the composition does not change over the face of the facet and run-to-run, a good assumption. The tabular results are given in thousands of counts per second and are not normalized.

The thickness uniformity across the facet is indicated by the data in Table 3-2 which shows the results for Run #1. The columns from left to right give the Sample Number, the Ag signal, the per cent deviation of the Ag signal from the mean, the Al signal, and the per cent deviation of the Al signal from the mean. The value reported as the mean is the mean of the sample population and does not represent the mean thickness of the coating averaged over the facet surface. These results show that the thickness uniformity within a single run was quite good. The largest Ag signal was 6.4% greater than the mean, and the smallest Ag signal was 4.8% less than the mean. The largest Al signal was 4.0% greater than the mean, and the smallest Al signal was 3.2% less than the mean.

The reproducibility of the thickness from run to run is indicated by the data in Table 3-3, which shows the results for five selected positions from three runs. For Ag the maximum variation at one point was 3.9%; for Al_2O_3 as Al 3.3%. The data point for position 20 in Run #2 is not given because that sample had been used for adhesion testing prior to analysis. The measurement had to be made through a piece of tape used for adhesion testing; the Ag result was good; but the Al result was not (due to attenuation of the lower energy Al Kα line).

A composite of the data is presented in Figures 3-23 and 3-24 for Ag and Al_2O_3 as Al, respectively. Note that the ordinate is expanded and does not include zero. The points are connected to aid the eye and should not be taken to imply linearity between points, especially for Runs #2 and #3. The abscissa in these figures is the coupon position number and represents a cut along a line through an apex of the facet perpendicular to an edge (see Figure 3-22). Figures 3-25 and 3-26 show the same data replotted with the distance from the center of the facet as the abscissa and the thickness normalized to unity at the thickest point. Both figures suggest that there are two branches for the data from the coupons in Run 1 on either side of the center. This effect is particularly evident in the Al data (Figure 3-26). This effect is thought to result primarily from errors in our coordinate representation. Again the uniformity and repeatability look good. The data suggest that the Al_2O_3 is more uniform than the Ag. This effect is due in part to the normalization procedure and what appears to be an overestimate of the thickness for the thickest Ag sample. Elimination of that error using the augen method (eye-balling it) does not eliminate all the discrepancy. The difference is likely due to slight differences in the evaporant flux distributions for Ag and Al_2O_3. The uniformity is expected to be quite acceptable functionally.

3.2.3.2 Thickness determination using ellipsometry

The ellipsometric determination of the dielectric thickness used a Gaertner Model L116 ellipsometer. The measurements were not performed on the system demonstration coupons. As noted above

separate runs were required to prepare the samples measured in this way. Eleven samples, from all even numbered positions 2 through 20 and position 1, were measured. The results are shown in Figure 3-27 as the actual thickness versus position and in Figure 3-28 as the relative thickness versus position. Again quite good uniformity is obtained. The large apparent variability associated with the Al_2O_3 film thickness is due to errors in the thickness measurement related to the thinness of the films.

3.2.3.3 Thickness determination using profilometry

A set of Ag films were prepared for thickness measurement using profilometry. An Alpha-Step 200 stylus profilometer was used. The errors associated with this measurement preclude using it for thickness uniformity studies for the films prepared here. Problems with the instrument and with substrate surface irregularities further reduced the value of these measurements. The average thickness of the ensemble of films prepared was approximately 60 nm. Later measurements on the Alpha-Step following repair by the manufacturer indicated an average thickness of 74 nm.

3.2.3.4 Reflectance uniformity

The reflectivities of the 30 coupons prepared were measured using a Perkin-Elmer Lambda 9 UV-VIS-NIR spectrophotometer with a 60mm integrating sphere. Total and diffuse reflectivities were measured as a function of wavelength. Specular reflectivities were calculated by difference. Integration over AMO to provide relative specular and relative total solar reflectivities were calculated using a program modified from a one supplied by D. A. Gulino, the NASA Project Manager. The modifications were made to adapt the program to our computer and style. The calculations were not changed. Identical data sets gave equal results as expected.

The total and specular reflectance uniformity results for the 30 coupons are plotted in Figures 3-29 and 3-30, respectively. As expected the uniformity and repeatability are quite good. There are at least two coupons (Run 1, Positions 4 and 10) with noticeably poorer results than the others. These poor results were found to be due to lower quality surfaces in the particular coupons which were used in those positions. There is a suggestion in the data in these figures when compared to Figure 3-23 that there is a slight increase in the reflectivity for coupons with thicker Ag coatings. See Section 3.2.3.6.

3.2.3.5 Adhesion promoter studies

Evaluation of the coupons for adhesion demonstrated that the use of Al_2O_3 as an adhesion promoter was not effective for quartz substrates. Earlier work had demonstrated adequate adhesion using

Al_2O_3. A small effort to develop techniques and/or materials which would provide adequate adhesion for the silver film was proposed and approved by the NASA Project Manager.

Further work using Al_2O_3 deposited under a variety of conditions as the adhesion promoter was not successful. Thin chromium was found to be effective on quartz but not on graphite-epoxy substrates (provided by Hercules). Thin copper was found to be effective on graphite-epoxy but not on quartz substrates. Preliminary tests showed that the copper did not affect the reflectance measured, that the adhesion and reflectivity were good after extended aging, and thermal annealing (150°C for 64 hours). Using available graphite-epoxy substrates, samples with copper under the protected silver failed our asher tests after short (24 hour) exposure times. The samples prepared on quartz with chromium adhesion promoter survived the asher with good reflectivities. A brief effort to determine the effect of copper film thickness on adhesion and reflectivity using copper films 2.5, 6.5 and 17 nm thick showed no detectable effect.

On presenting this information to D. A. Gulino, we agreed that NASA would provide graphite-epoxy samples for coating with copper followed by the standard protected silver film. The samples were prepared and delivered to NASA-LeRC for AO durability testing. The results of the testing are shown in a graph supplied by D. A. Gulino and included here as Figure 3-31.

3.2.3.6 Effect of film thickness on specular reflectance

An attempt to show that the specular reflectance (on graphite epoxy substrates with imperfect surfaces) would increase by using thicker metal coatings (to fill in the cracks) was successful. As better quality substrates become available this test should be repeated. Thin films are thought to replicate the contours of the substrate on which they are coated. For most regimes this is demonstrably true. In order for a thin film to change the surface contour, some of the surface features must have dimensions near the value of the film thickness, and the atoms deposited must have some level of mobility of the substrate surface.

To test this effect ten square samples of graphite epoxy (Hercules) were each marked and cut into two rectangular pieces. One piece of each pair was coated with 70 nm aluminum; the other piece was coated with 200 nm aluminum. After coating, the diffuse reflectance of each of the 20 pieces was determined. Diffuse reflectance is a good indicator of surface quality for the surfaces examined here. Care was taken to measure the %R near the common boundary between the original pairs of pieces. This strategy was an attempt to minimize the effect of changes in surface quality over the surface of the graphite epoxy.

The mean values (and standard deviation) for R_d was 2.5 (0.7) for the 200nm coating and 3.3 (1.3) for the 70nm coating. Eliminating the two worst samples (as measured by the difference between the R_d values for the 70 and 200nm samples) gave 2.4 (0.7) and 2.8 (1.0). The large standard deviations are associated with the variation in the surface quality of the graphite epoxy. Statistically the mean values differ by less than the standard deviations. No firm conclusion could have been drawn from the data without the pairing noted above.

However having kept track of the sample pairs, it is possible to note that eight of ten showed lower R_d with the 200 nm coating than the 70 nm coating. The average value (and standard deviation) of the differences in per cent diffuse reflectance was 0.8 (0.8). Eliminating the two worst samples noted above the average value of the difference was 0.4 (0.4). The statistical basis of this procedure is discussed in many textbooks.[10] This result indicates that increasing the metal thickness would increase the specular reflectivity for Al coated graphite-epoxy substrates by 0.4%. Clearly the magnitude of this effect should be determined using the full four layer construction and the graphite-epoxy substrates planned for flight hardware when they become available.

3.2.4 Subtask 2.4 Coating of an Indefinite Number of Facets

At the time of this report the last objective, the coating of an indefinite number of facets, was an option not yet exercised by NASA.

4 HARRIS SUBCONTRACT EFFORT

The Harris subcontract effort was crucial to the success of this program. The system design and materials preparation and testing information developed as part of the Solar Collector Advanced Development Program[1] provided a vital input to this effort. Much of the Harris effort related to information transfer and assistance in development of an appropriate context wherein this effort could be effective. Additionally Harris personnel provided graphite-epoxy coupons for testing with the coating developed here when quality graphite-epoxy substrates were otherwise unavailable.

5 RECOMMENDATIONS FOR FURTHER WORK

During the course of the work described above a number of issues arose which were relevant to this work but were not addressed either because they were not part of the funded effort or because they were experimentally unaddressable at the time of the effort. These issues have all been discussed in the body of the report but are noted here for convenience.

The graphite-epoxy substrates available at the time of this effort were unacceptable and required improvements in the surface finish in the areas of smoothness and defects and/or contaminants. Specifically the lifetime of coated epoxy-graphite coupons in atomic oxygen tests were unacceptable, and the specular reflectivity of coated coupons was reduced due to surface deficiencies. Tests of the atomic oxygen durability and adhesion of the $Cu/Ag/SiO_2/Al_2O_3$ coatings on graphite-epoxy substrates suitable for flight hardware are recommended. Given acceptable lifetimes, the durability of the coatings as a function of thickness of the layers might also be considered. The dependence of the specular reflectivity on Ag thickness should be determined to optimize the Ag thickness.

The effects of actual LEO exposure should be determined or simulated as more flight time and better simulation tests become available. Tests should simulate AO, thermal cycling, UV, and micrometeoroid exposure. The tests to determine the effects of UV exposure should look specifically at wavelengths near 320 nm where silver is partially transparent. The effects of particulate defects on the facet surface before coating have not be evaluated (although initial asher testing has shown no catastrophic effects).

Finally the coatings applied under this effort protect the front surface of the graphite-epoxy facet. The rear surface and the edges also require protection.

TABLES

Table 3-2

Position	Ag Kα	% Deviation	Al Kα	% Deviation
1	5.62	1.33	7.61	0.48
2	5.78	4.21	7.82	3.25
3	5.90	6.37	7.88	4.04
4	5.80	4.57	7.84	3.51
5	5.72	3.13	7.84	3.51
6	5.75	3.67	7.79	2.85
7	5.63	1.51	7.70	1.66
8	5.54	-0.12	7.63	0.74
9	5.44	-1.92	7.55	-0.32
10	5.42	-2.28	7.48	-1.24
11	5.34	-3.72	7.43	-1.90
12	5.40	-2.64	7.40	-2.30
13	5.32	-4.08	7.39	-2.43
14	5.28	-4.80	7.33	-3.22
15	5.36	-3.36	7.38	-2.56
16	5.40	-2.64	7.41	-2.17
17	5.41	-2.46	7.43	-1.90
18	5.55	0.06	7.45	-1.64
19	5.63	1.51	7.55	-0.32
20	5.64	1.69	7.57	-0.05
Mean =	5.55		7.57	

Table 3-3

Ag Kα

Position	Run #1	Run #2	Run #3	% Variation
1	5.62	5.59	5.55	0.71
5	5.72	5.80	5.66	2.45
10	5.42	5.47	5.26	3.87
15	5.36	5.41	5.24	3.17
20	5.64	5.78	5.64	2.48

Al Kα

Position	Run #1	Run #2	Run #3	% Variation
1	7.61	7.36	7.56	-3.29
5	7.84	7.62	7.66	2.30
10	7.48	7.39	7.35	1.74
15	7.38	7.29	7.32	-1.22
20	7.57	NA	7.62	NA

REFERENCES

1. NASA Report Number CR-179489, "Solar Collector Advanced Development Program Task 1 Final Report," prepared by Harris Corporation.

2. See D. A. Gulino, R. A. Egger and W. F. Banholzer, NASA Report Number TM-88865, "Oxidation-resistant reflective surfaces for solar dynamic power generation in near earth orbit," 1986; and Paragraph 7.0 "Materials Evaluation" in NASA Report Number CR-179489, "Solar Collector Advanced Development Program Task 1 Final Report," prepared by Harris Corporation.

3. D. A. Gulino, NASA Report Numbers TM-88874, "Effect of hard particle impacts on the atomic oxygen survivability of reflector surfaces with transparent protective overcoats," 1987, and TM-88914, "The survivability of large space-borne reflectors under atomic oxygen and micrometeoroid impact," 1987.

4. H. E. Bennett and J. M. Bennett, Physics of Thin Films 4, 1 (1967).

5. R. B. Pettit and E. P. Roth, in "Solar mirror materials: their properties and uses in solar concentrating collectors," in Solar Materials Science, L. E. Murr, ed., pg 171 (Academic Press, NY, 1980).

6. H. E. Bennett and J. L. Stanford, J. Res. Nat'l Bur. Stds. 80A, 643 (1976).

7. L. J. Cunningham and A. J. Braundmeier, Jr., Phys. Rev. B14, 479 (1976).

8. H. E. Bennett and J. L. Stanford, J. Res. Nat'l Bur. Stds. 80A, 643 (1976).

9. H. E. Bennett and J. M. Bennett, Physics of Thin Films 4, 1 (1967).

10. See for example, G. E. P. Box, W. G. Hunter, and J. S. Hunter, "Statistics for Experimenters," p. 97. Wiley, New York, 1978.

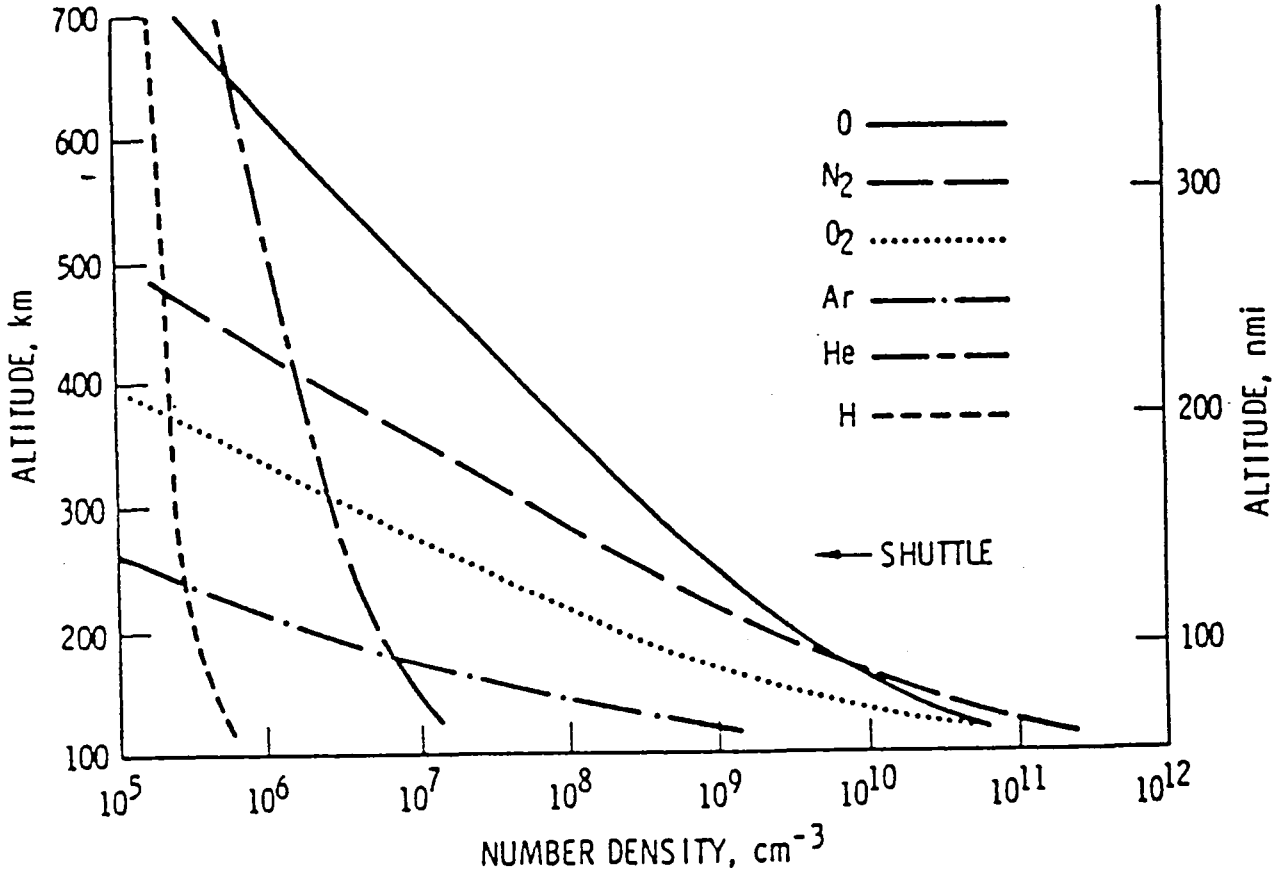

Figure 2-1 Atmospheric composition as a function of altitude.

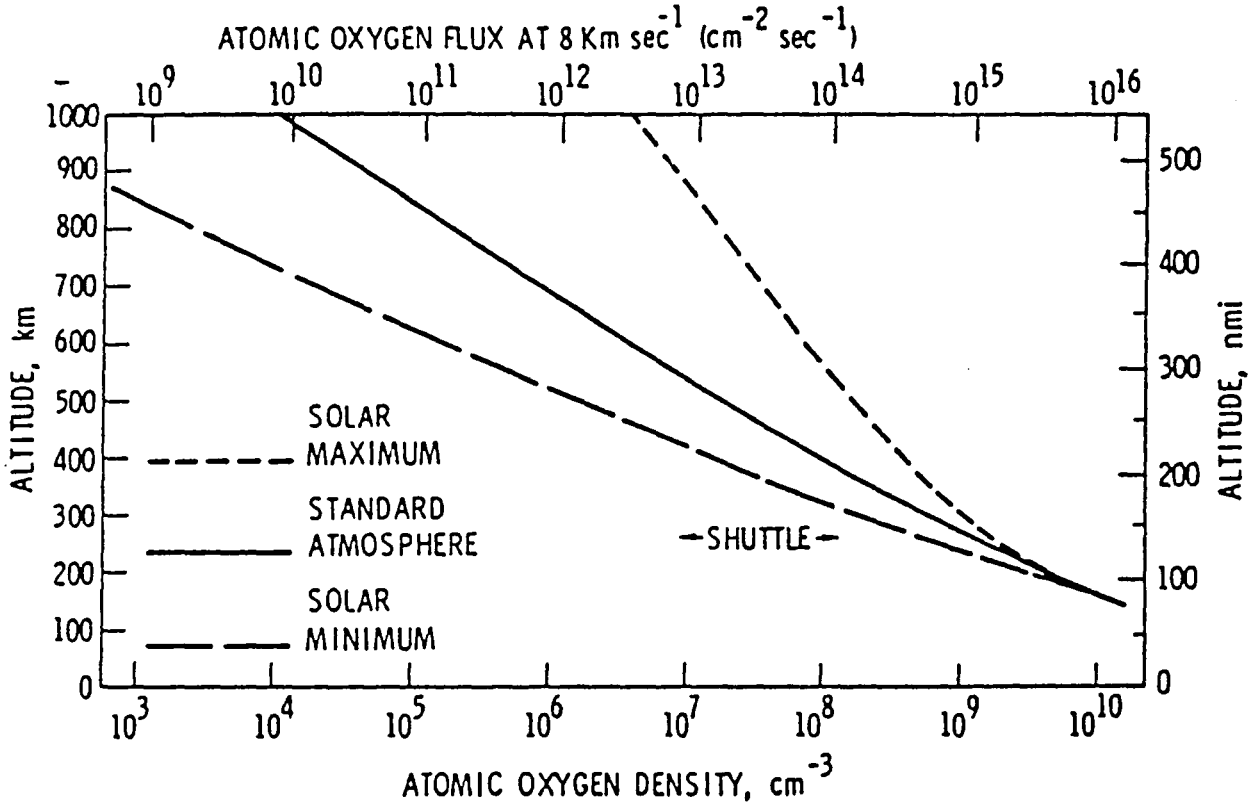

Figure 2-2 Atomic oxygen density and flux as a function of altitude.

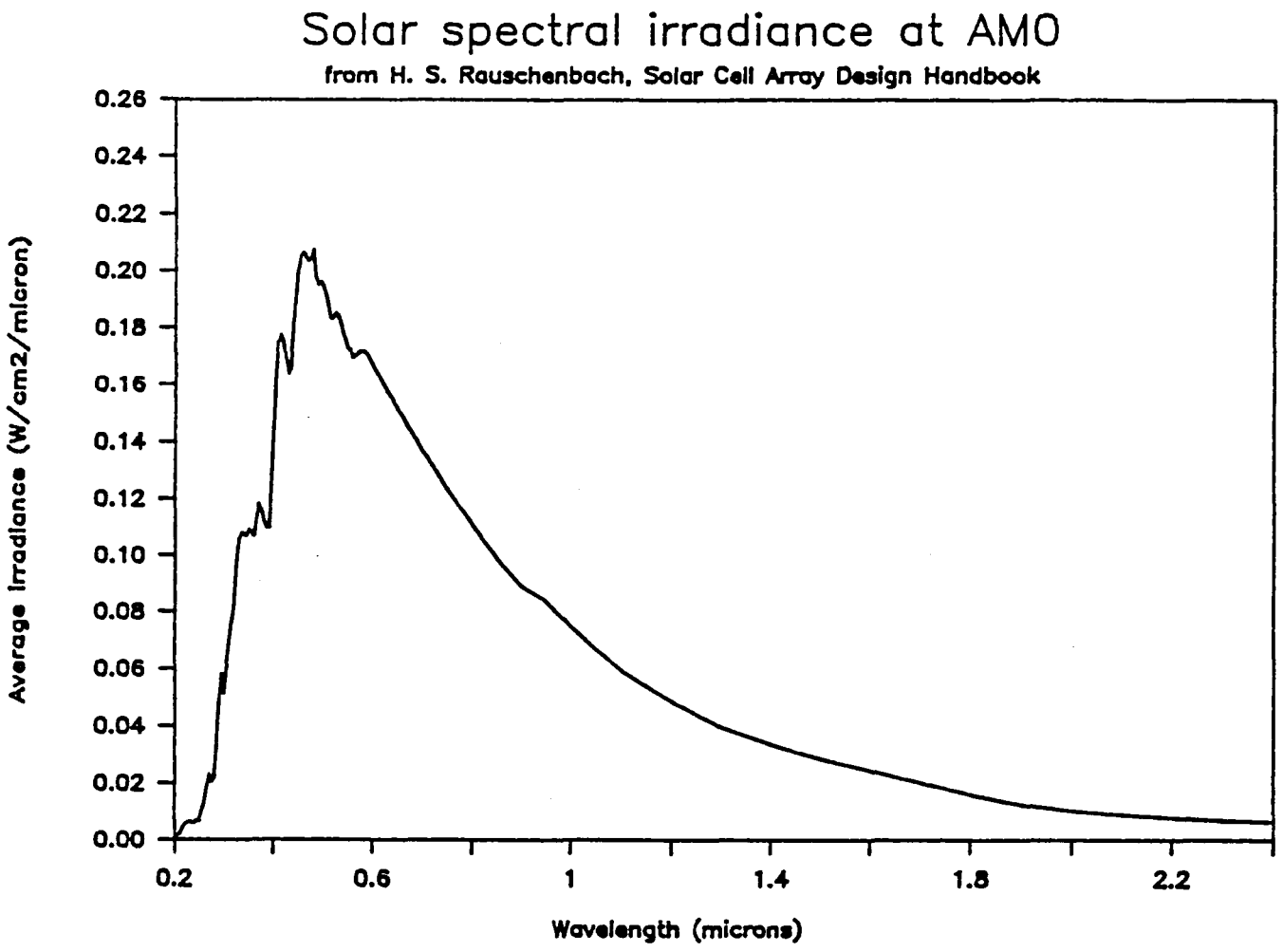

Figure 2-3 Relative solar spectral irradiance at air mass zero.

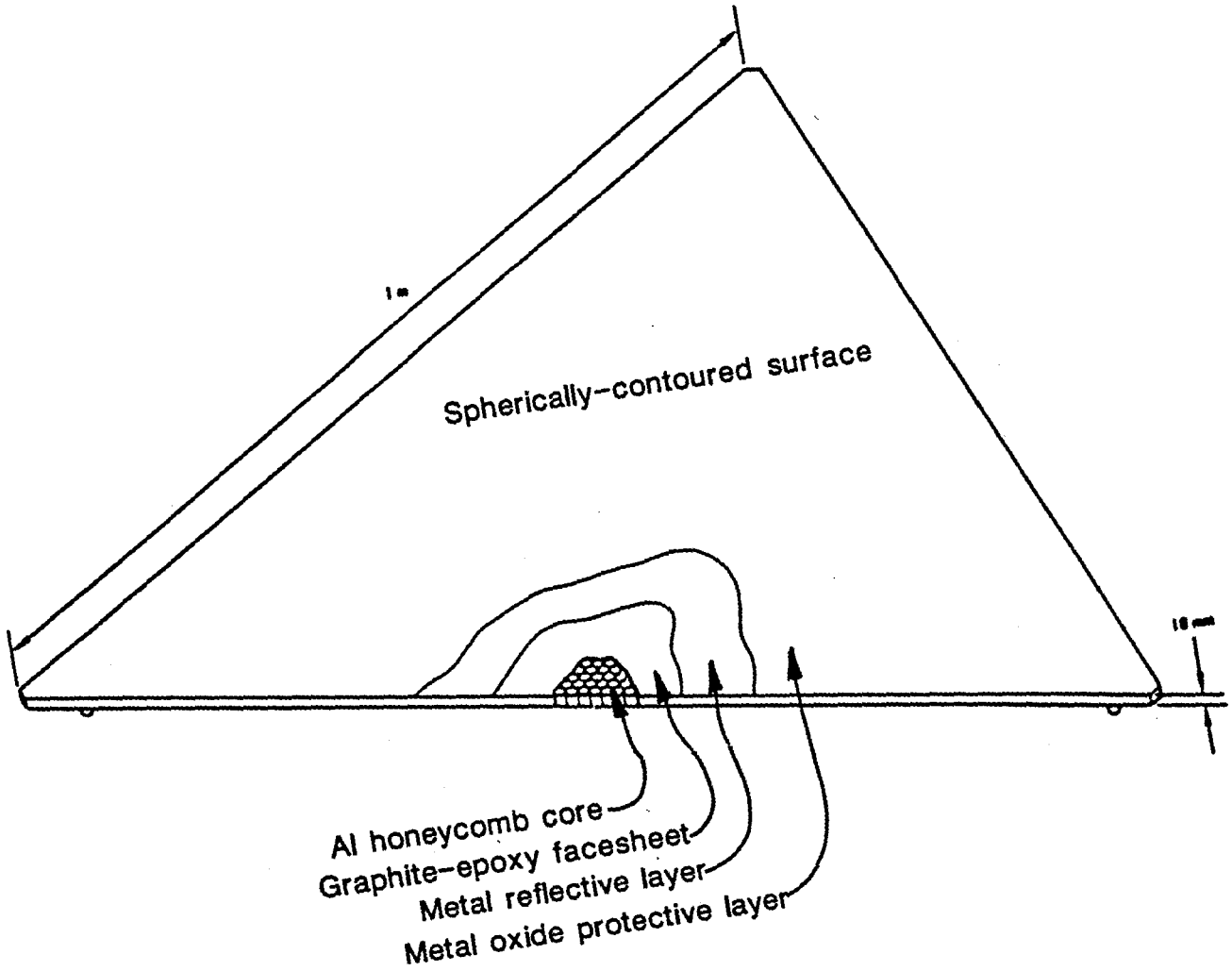

Truss Hex Mirror Facet

Figure 3-1 Schematic diagram of facet.

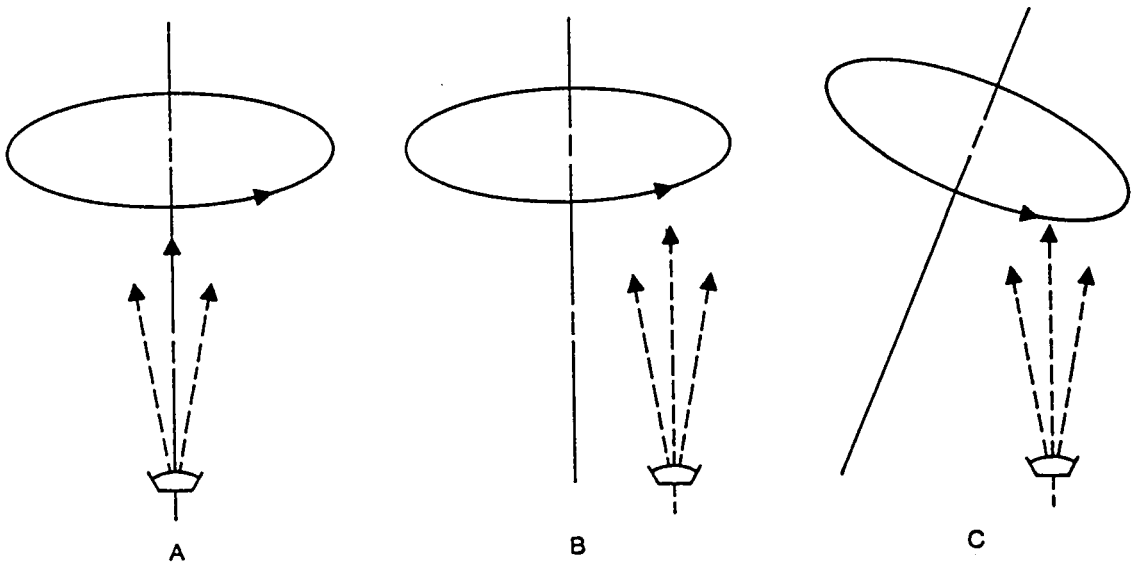

Figure 3-2 Coating geometries. The coating thickness uniformities calculated for these geometries are shown in Figure 3-3.

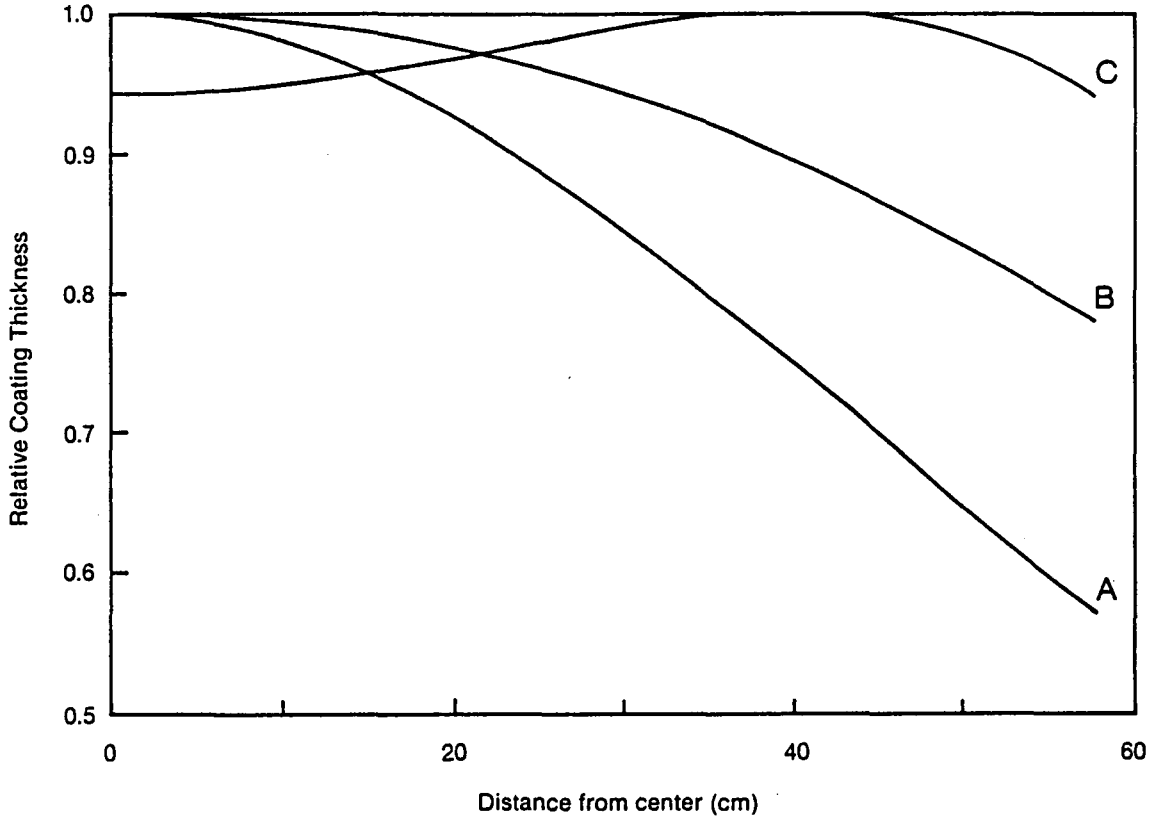

Figure 3-3 Coating thickness uniformities calculated for coating geometries shown in Figure 3-2.

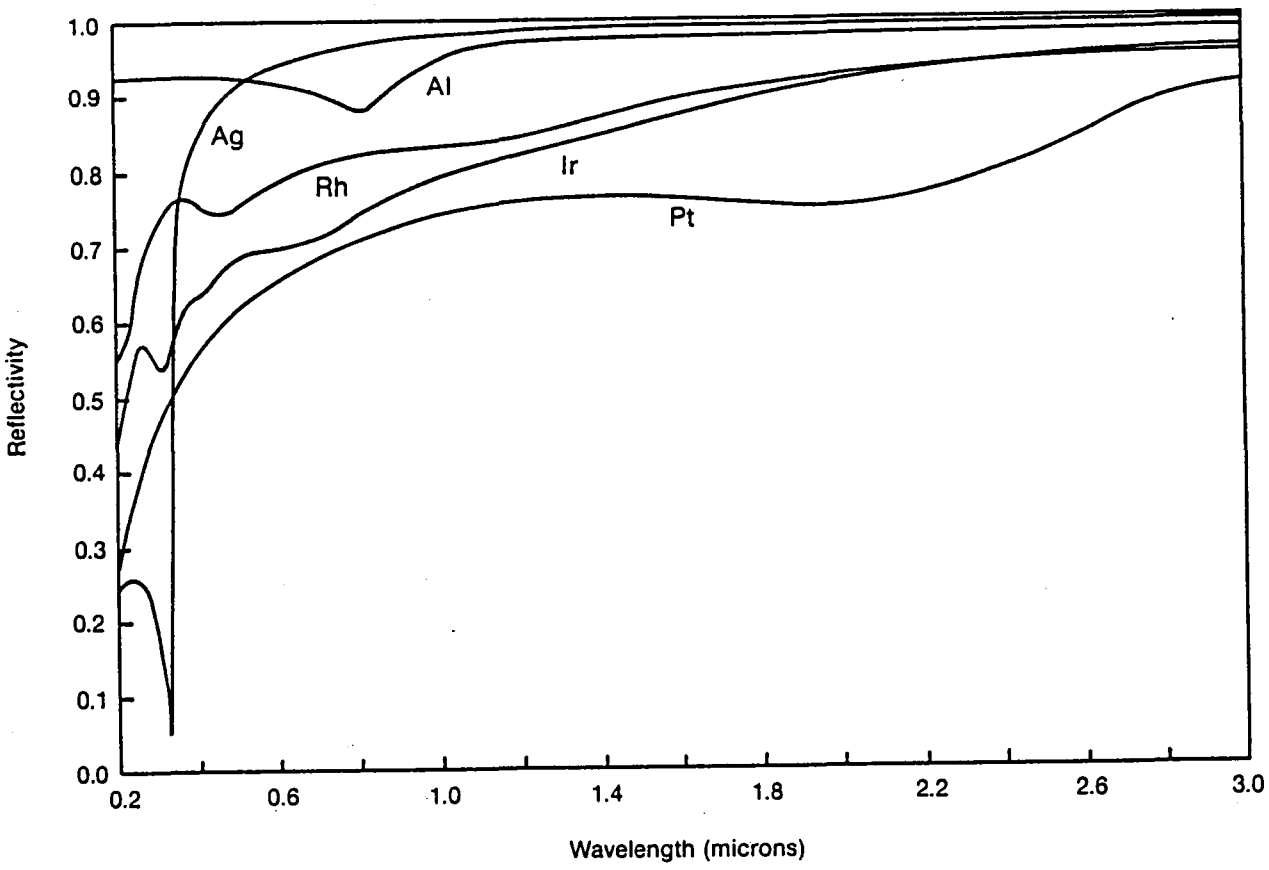

Figure 3-4 Reflectivity data for five metals as a function of wavelength.

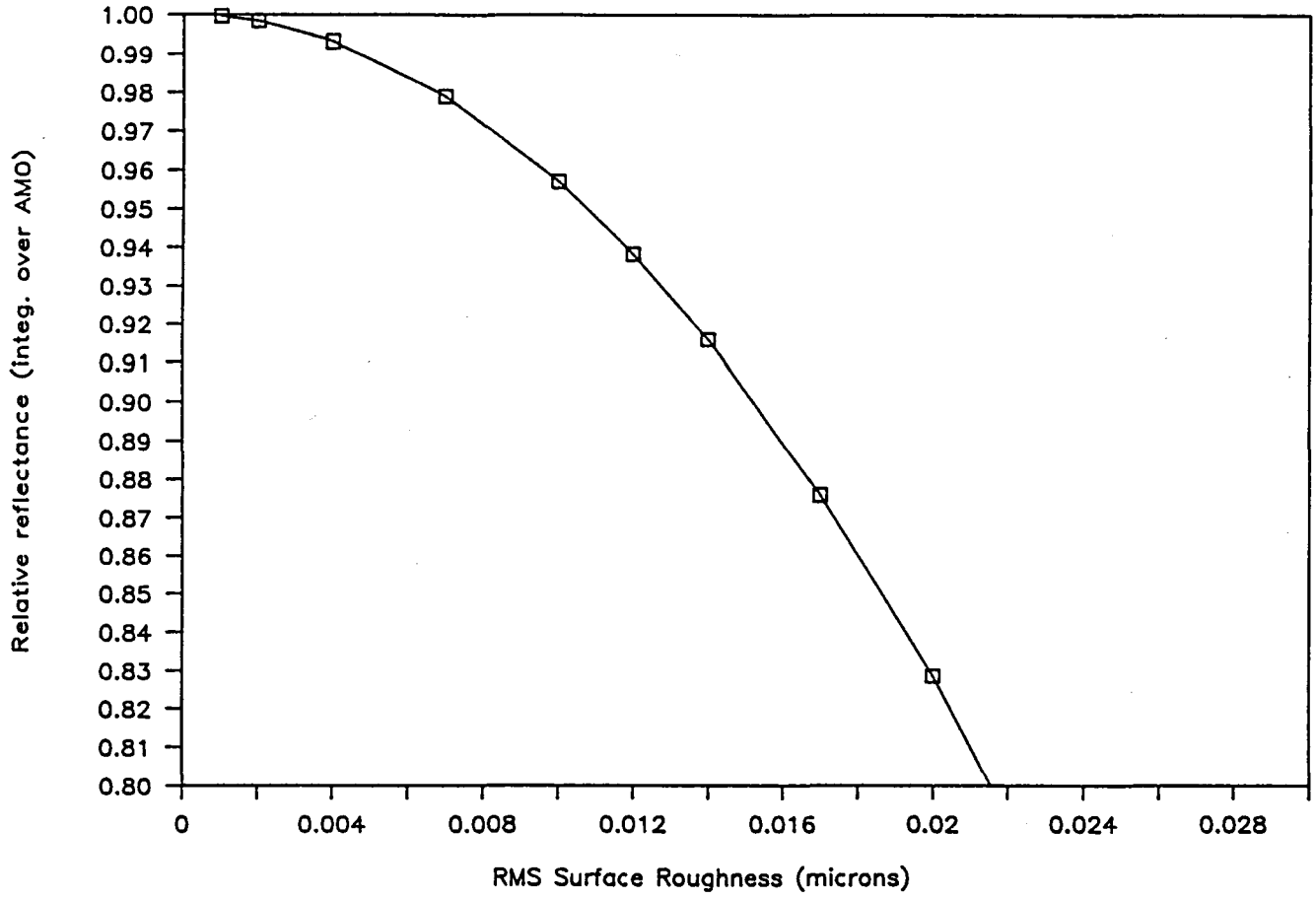

Figure 3-5 Results of model calculation of effect of surface roughness on specular reflectivity.

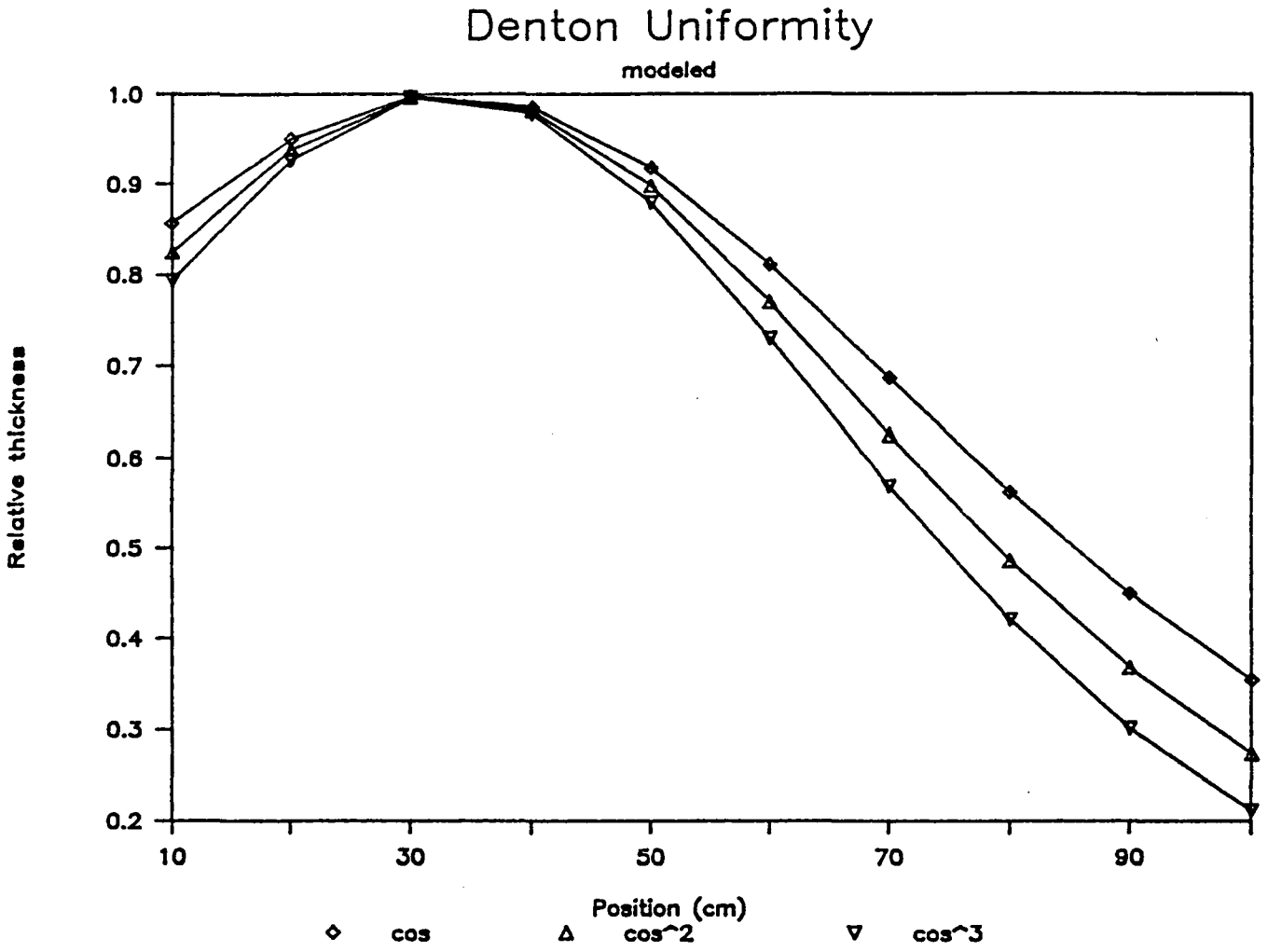

Figure 3-6 Calculated relative thickness values as a function of position for stationary substrates.

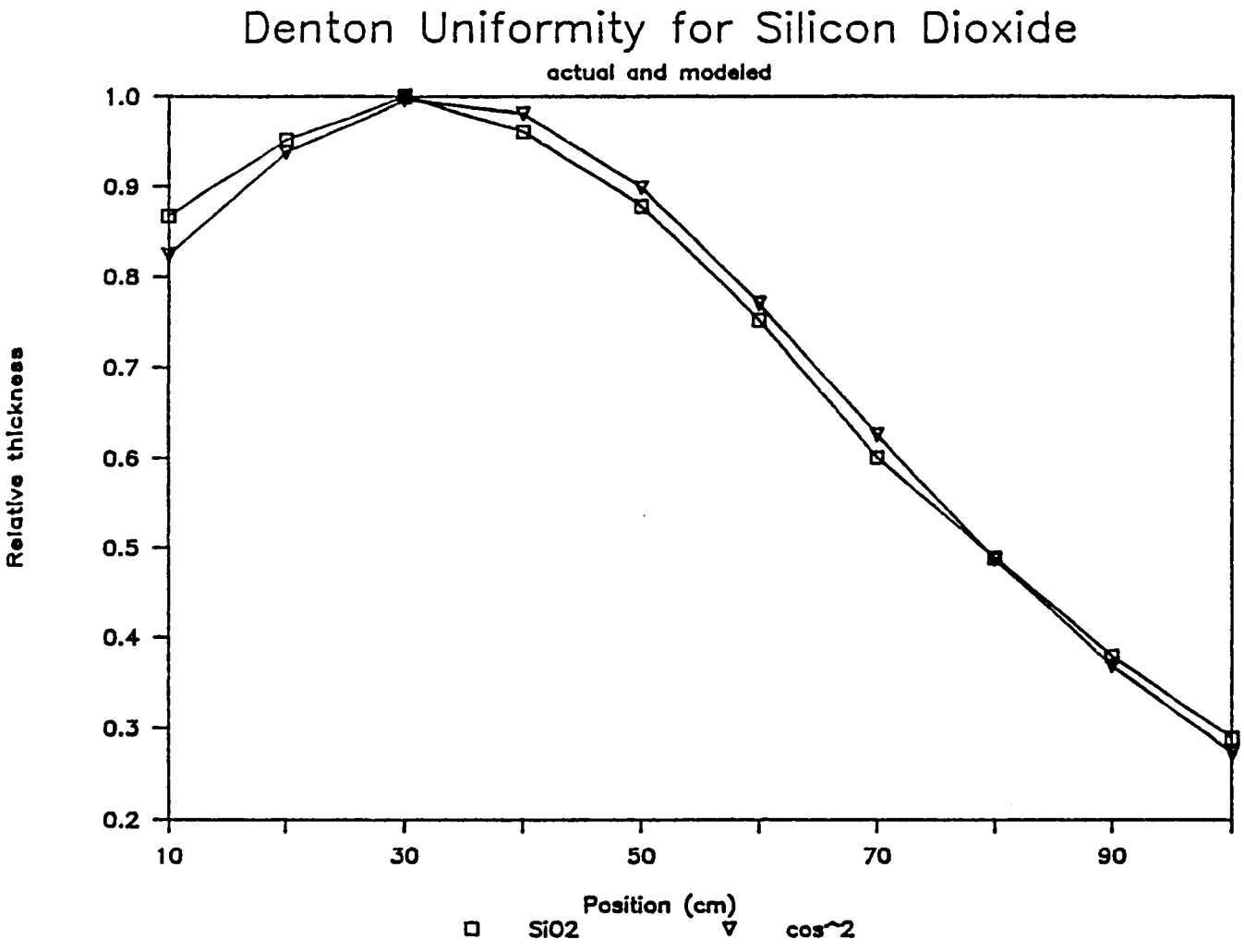

Figure 3-7 Measured relative thickness values as a function position for SiO_2.

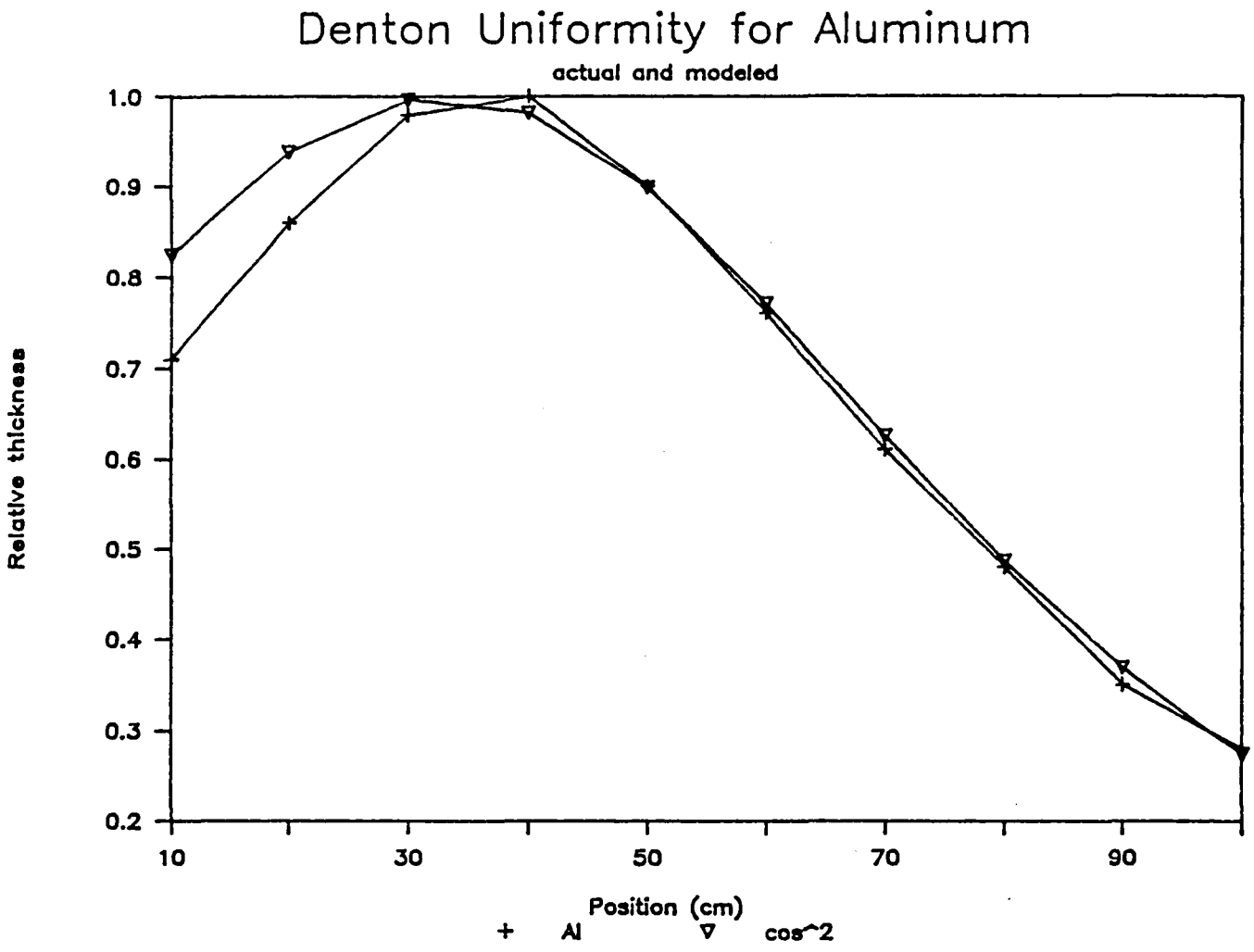

Figure 3-8 Measured relative thickness values as a function of position for Al.

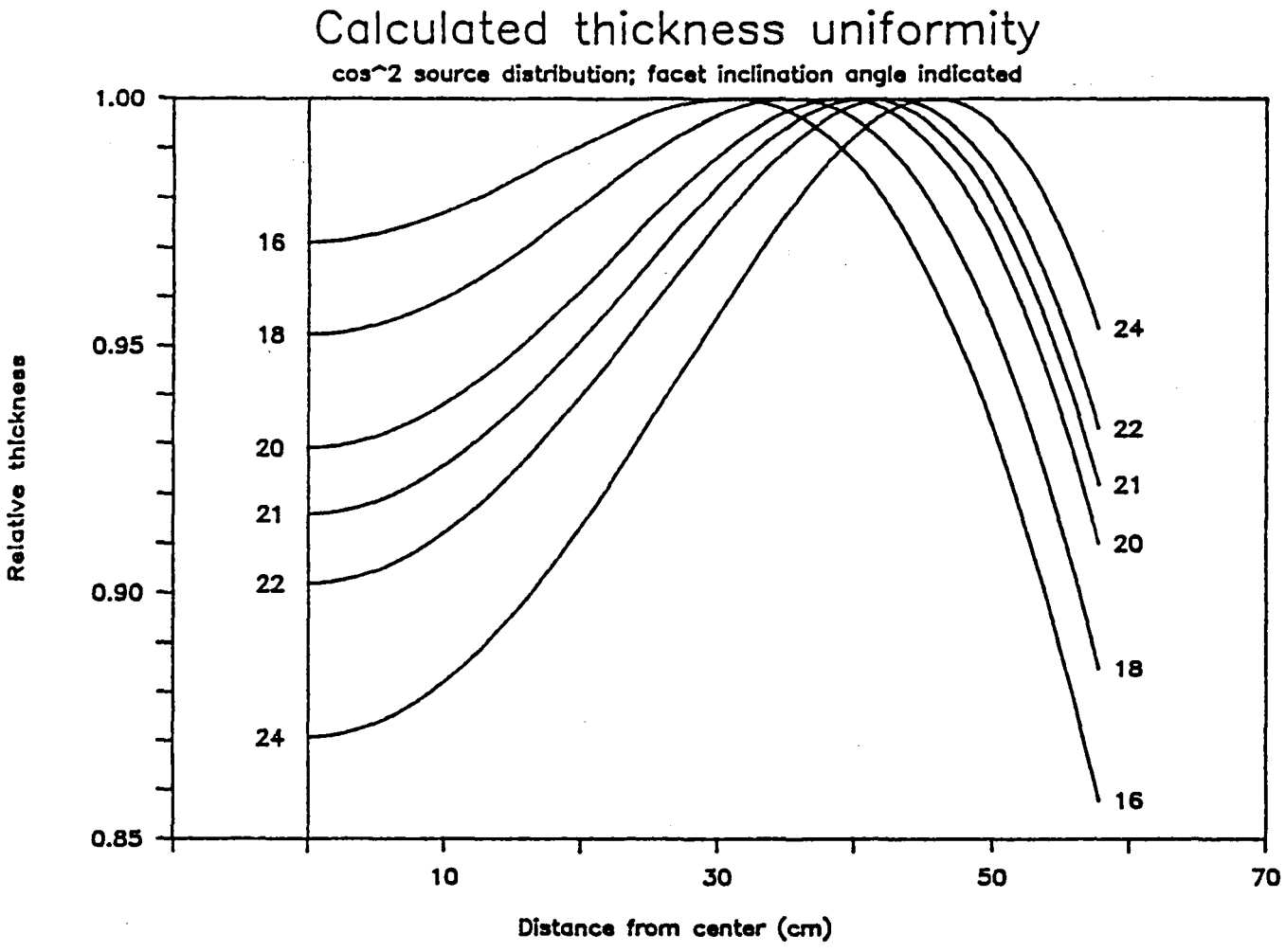

Figure 3-9 Thickness uniformity calculated for selected facet inclination angles.

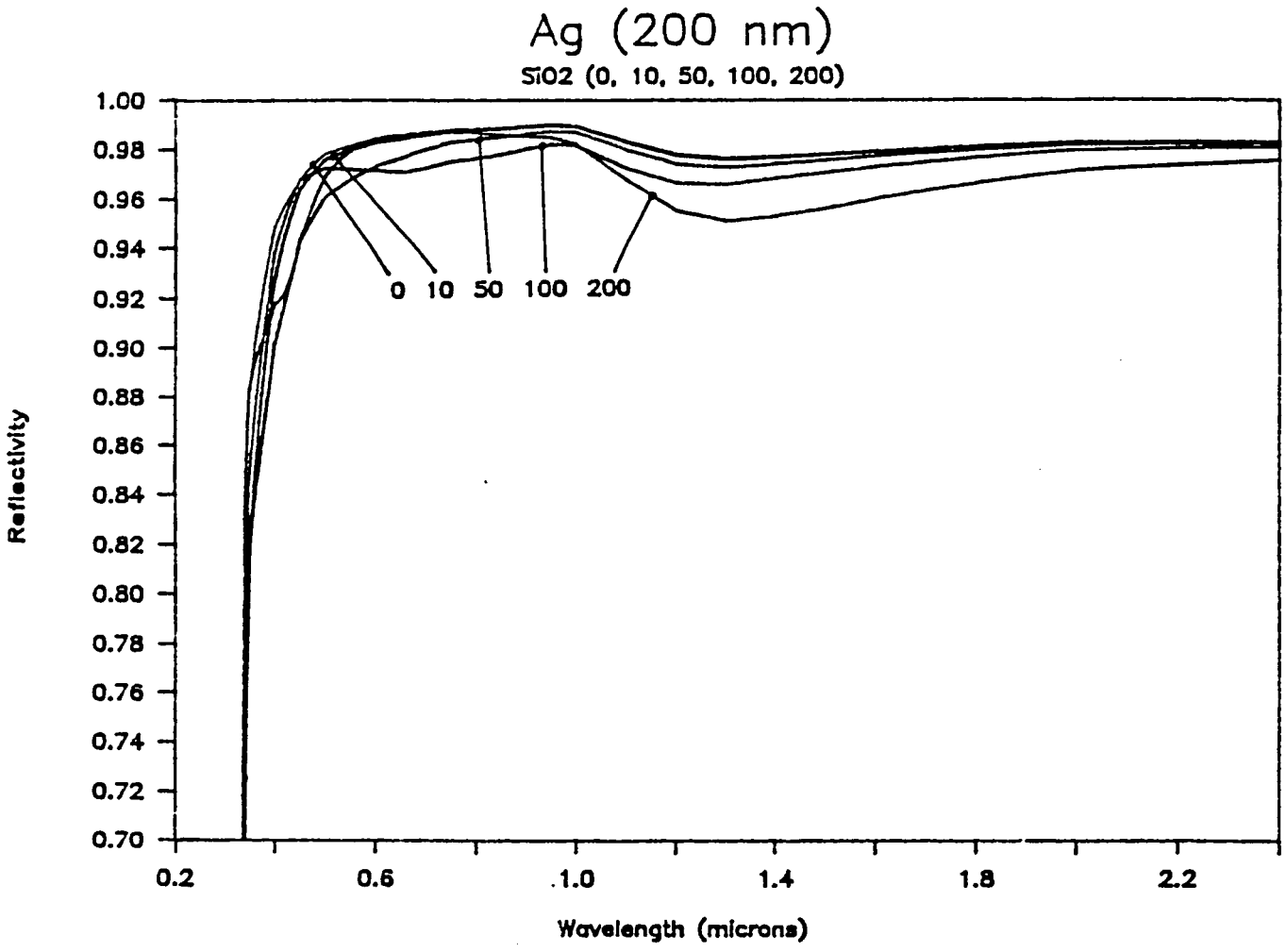

Figure 3-10 Reflectivity calculated as a function of wavelength for Ag with selected thicknesses of SiO_2 overcoats.

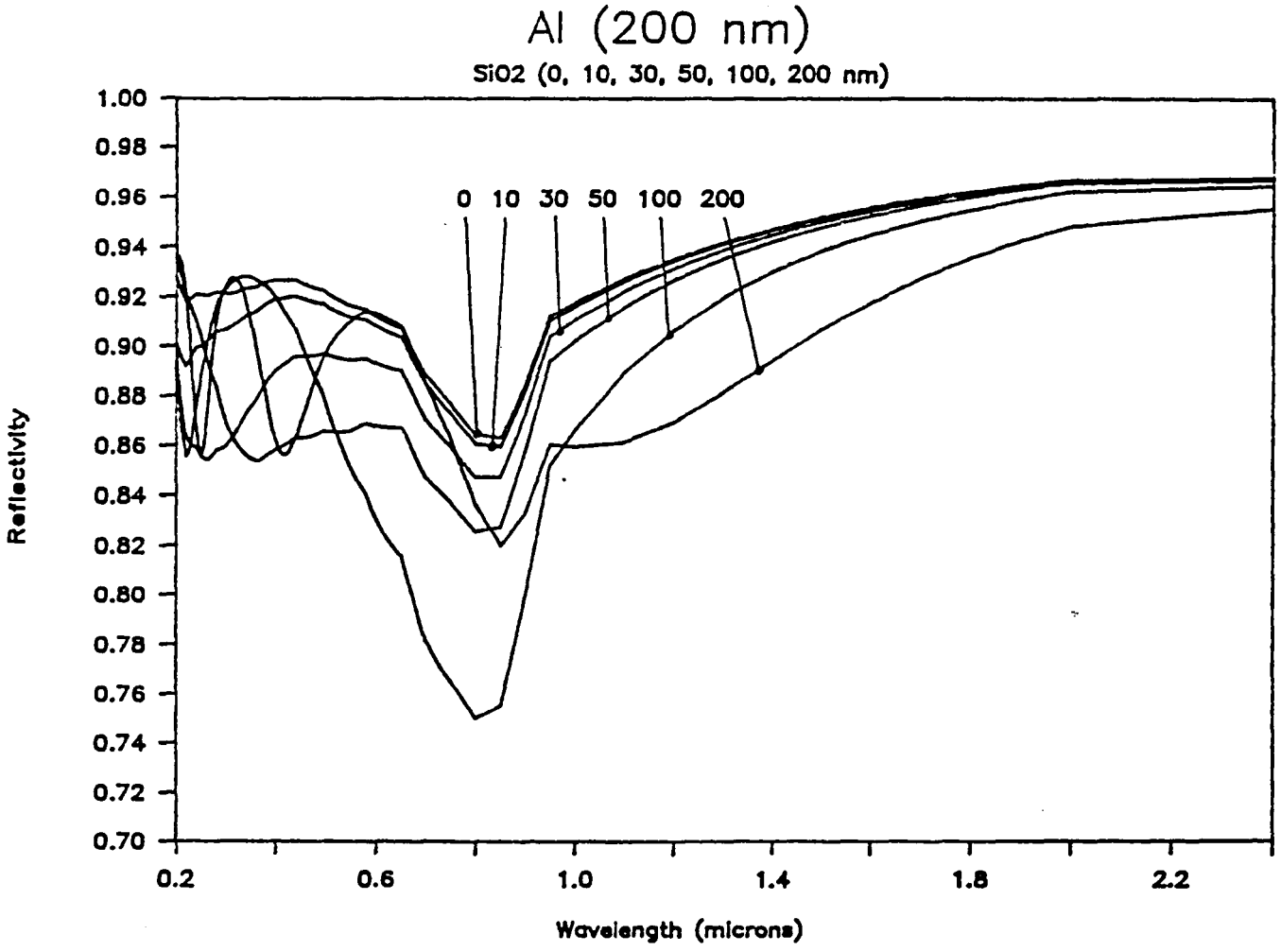

Figure 3-11 Reflectivity calculated as a function of wavelength for Al with selected thicknesses of SiO_2 overcoats.

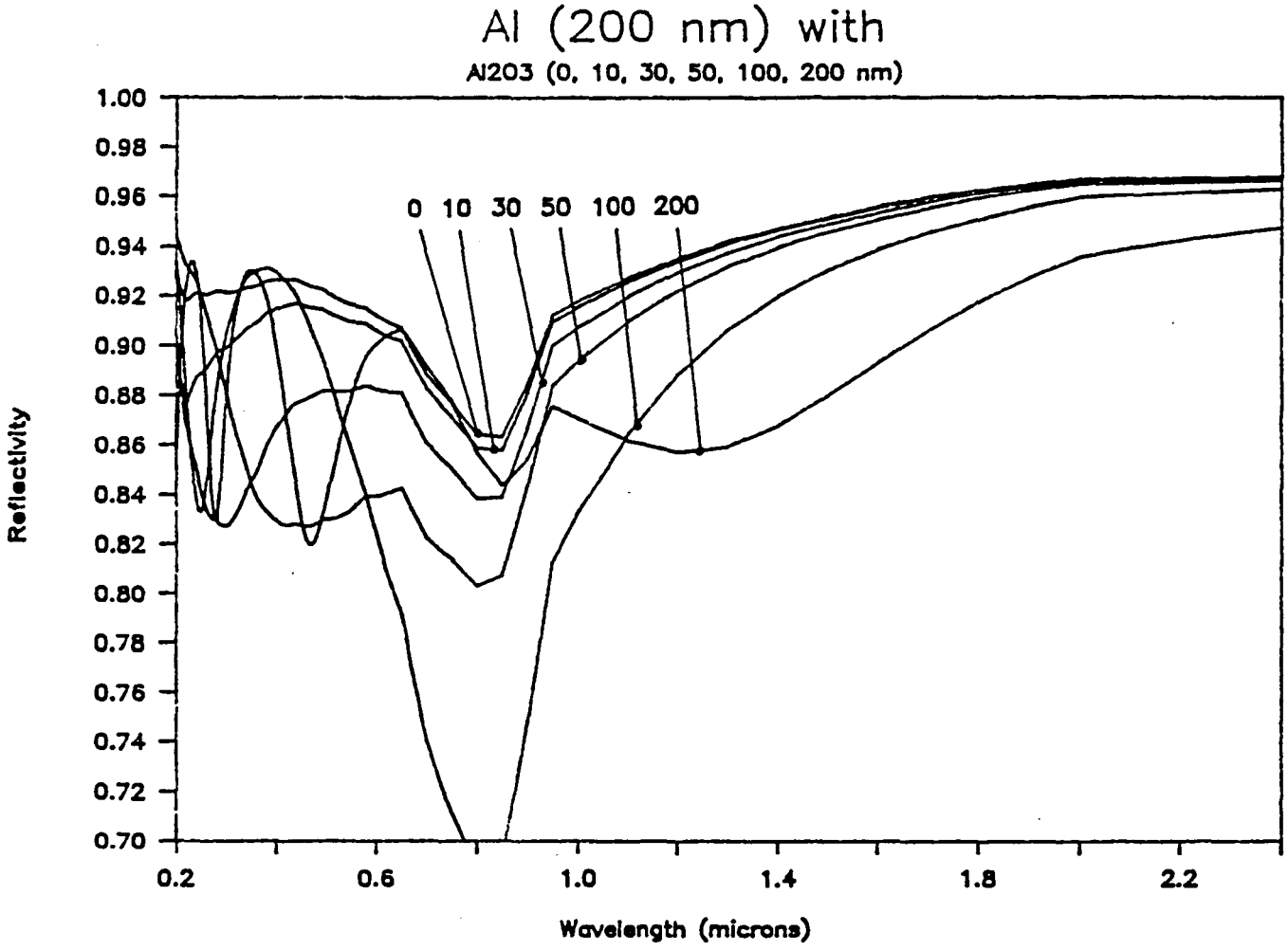

Figure 3-12 Reflectivity calculated as a function of wavelength for Al with selected thicknesses of Al_2O_3 overcoats.

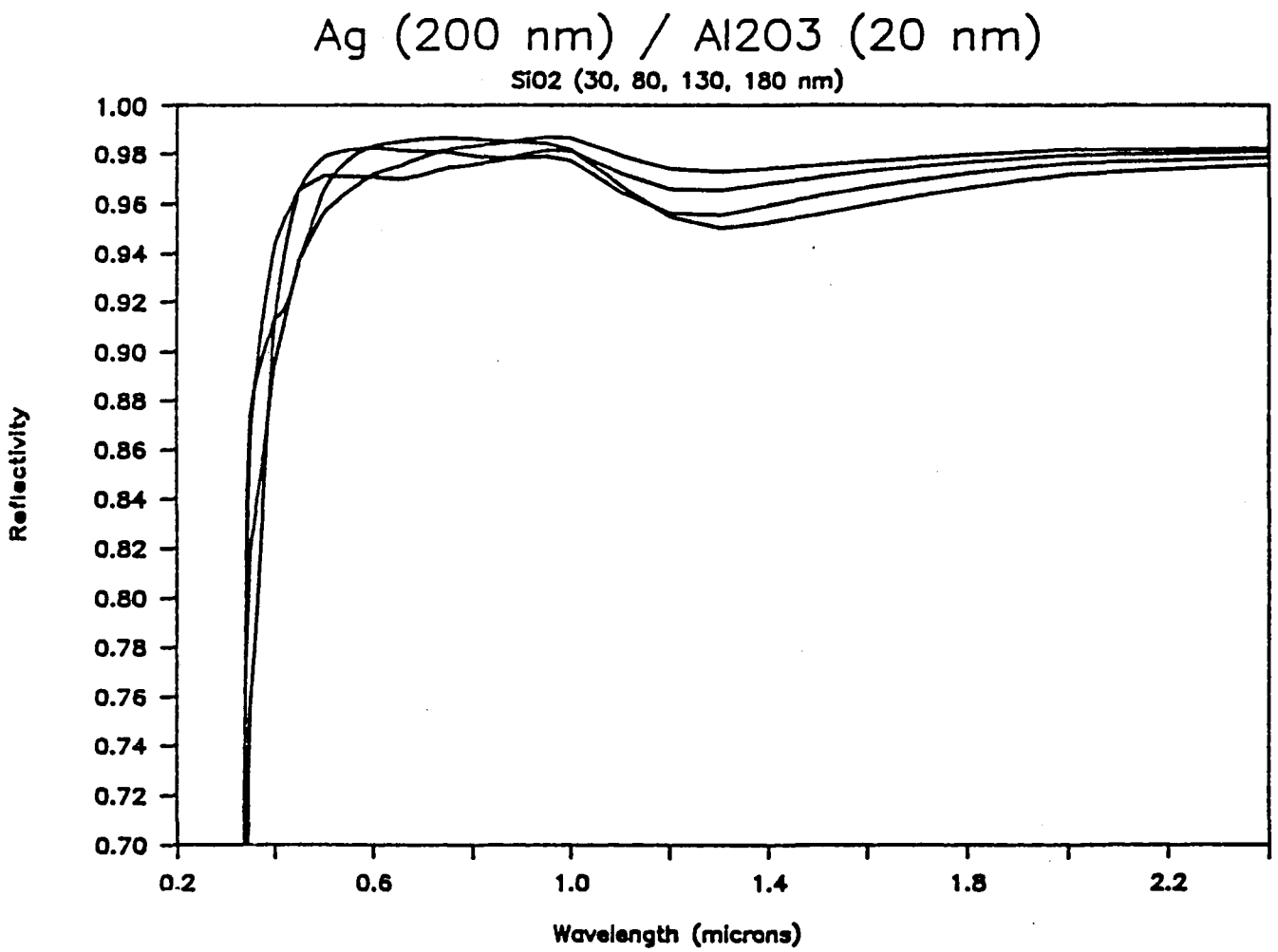

Figure 3-13 Reflectivity calculated as a function of wavelength for Ag with 20 nm of Al_2O_3 plus selected thicknesses of SiO_2 overcoats.

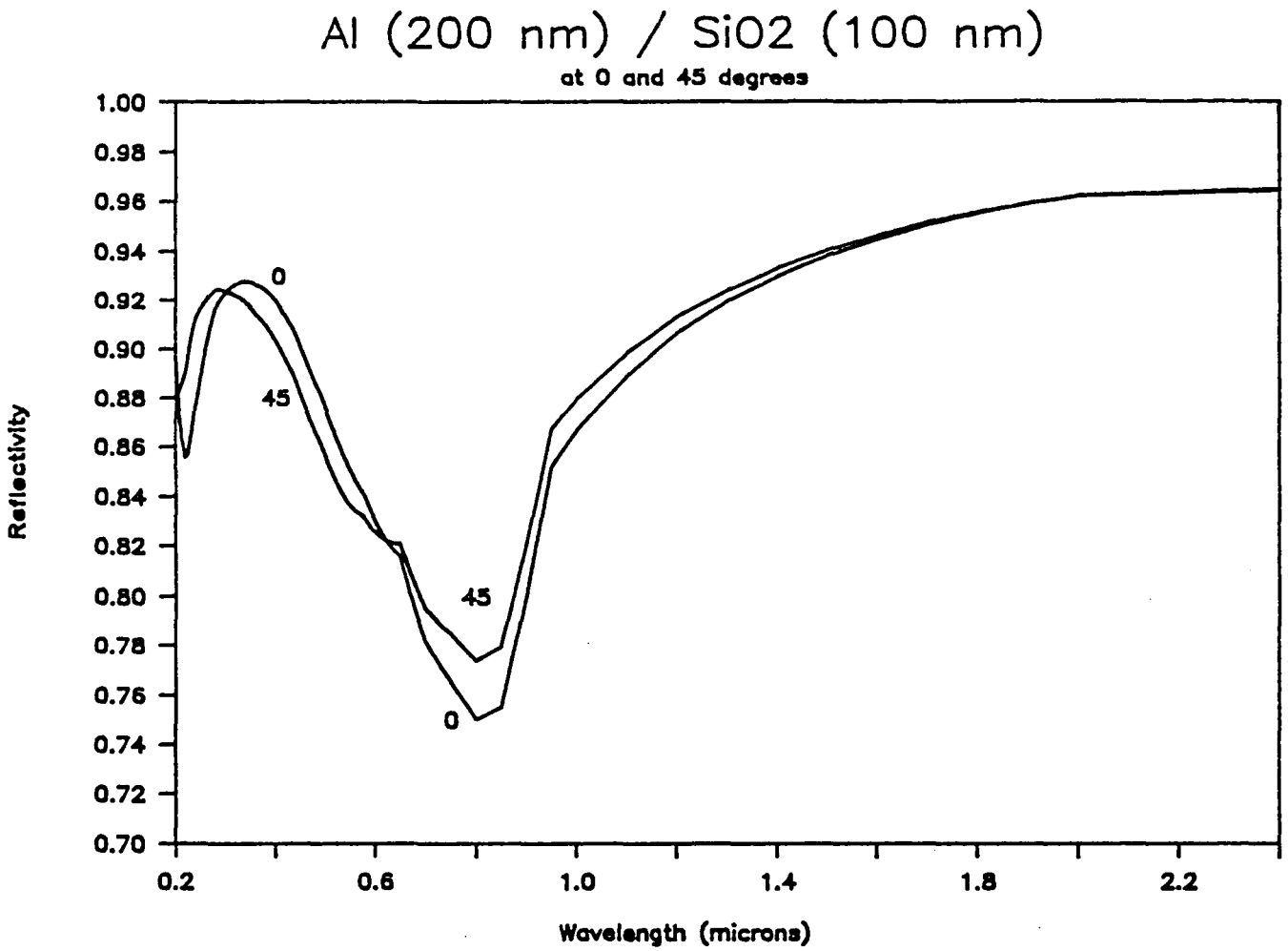

Figure 3-14 Effects of incidence angle on the reflectivity of overcoated Al.

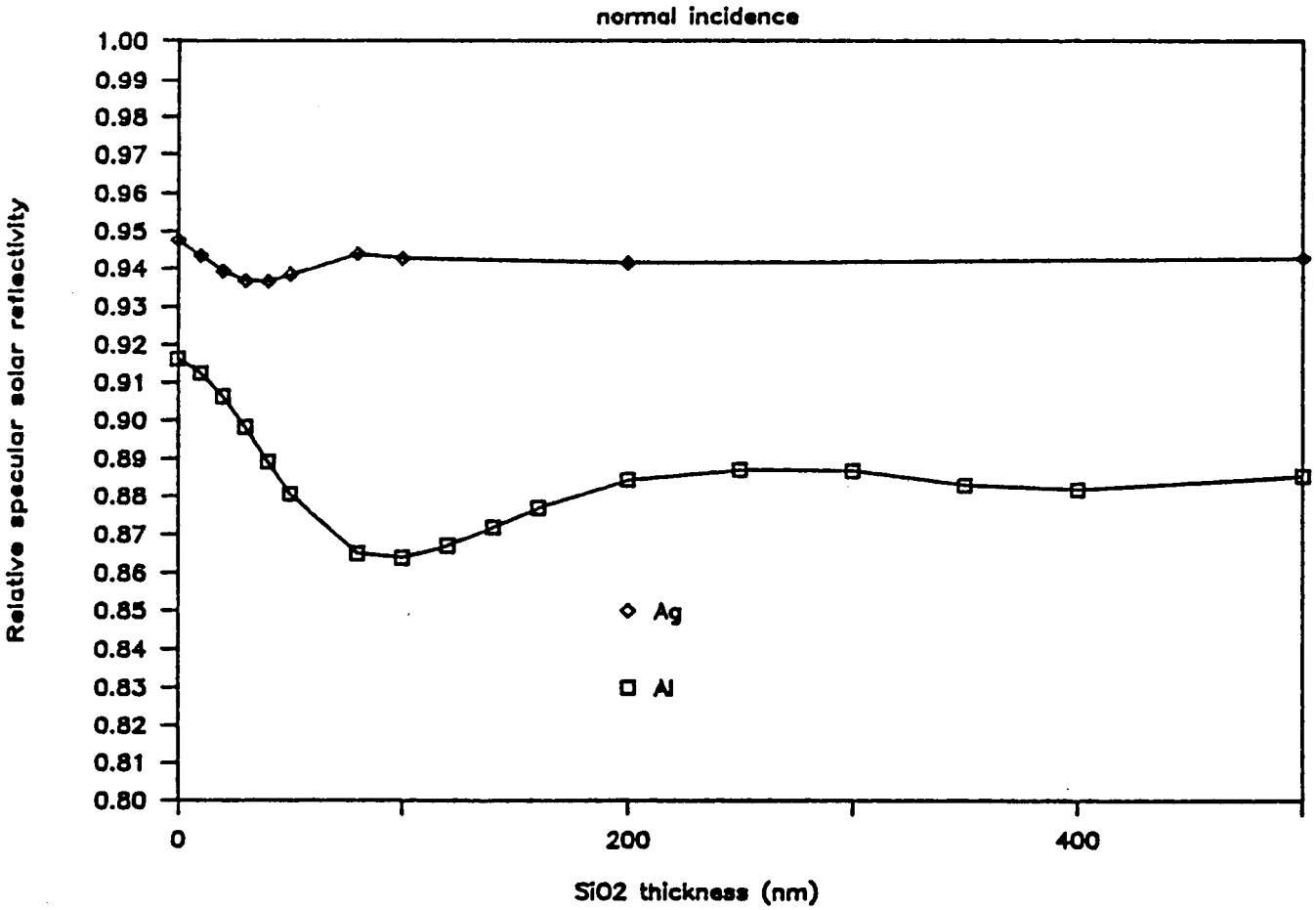

Figure 3-15 Calculated reflectance spectra averaged over AM0 for Ag and Al as a function of SiO_2 overcoat thickness.

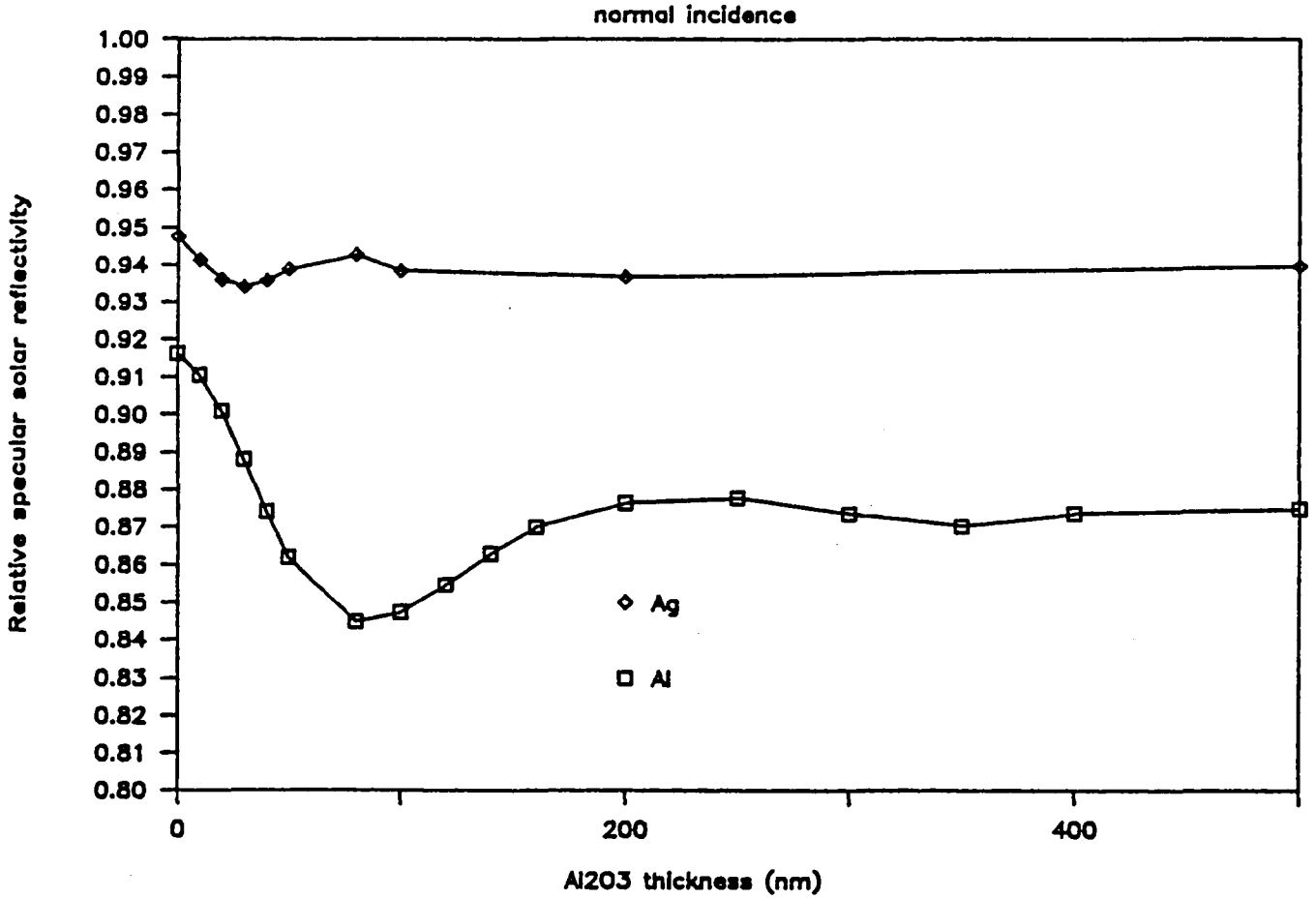

Figure 3-16 Calculated reflectance spectra averaged over AM0 for Ag and Al as a function of Al_2O_3 overcoat thickness.

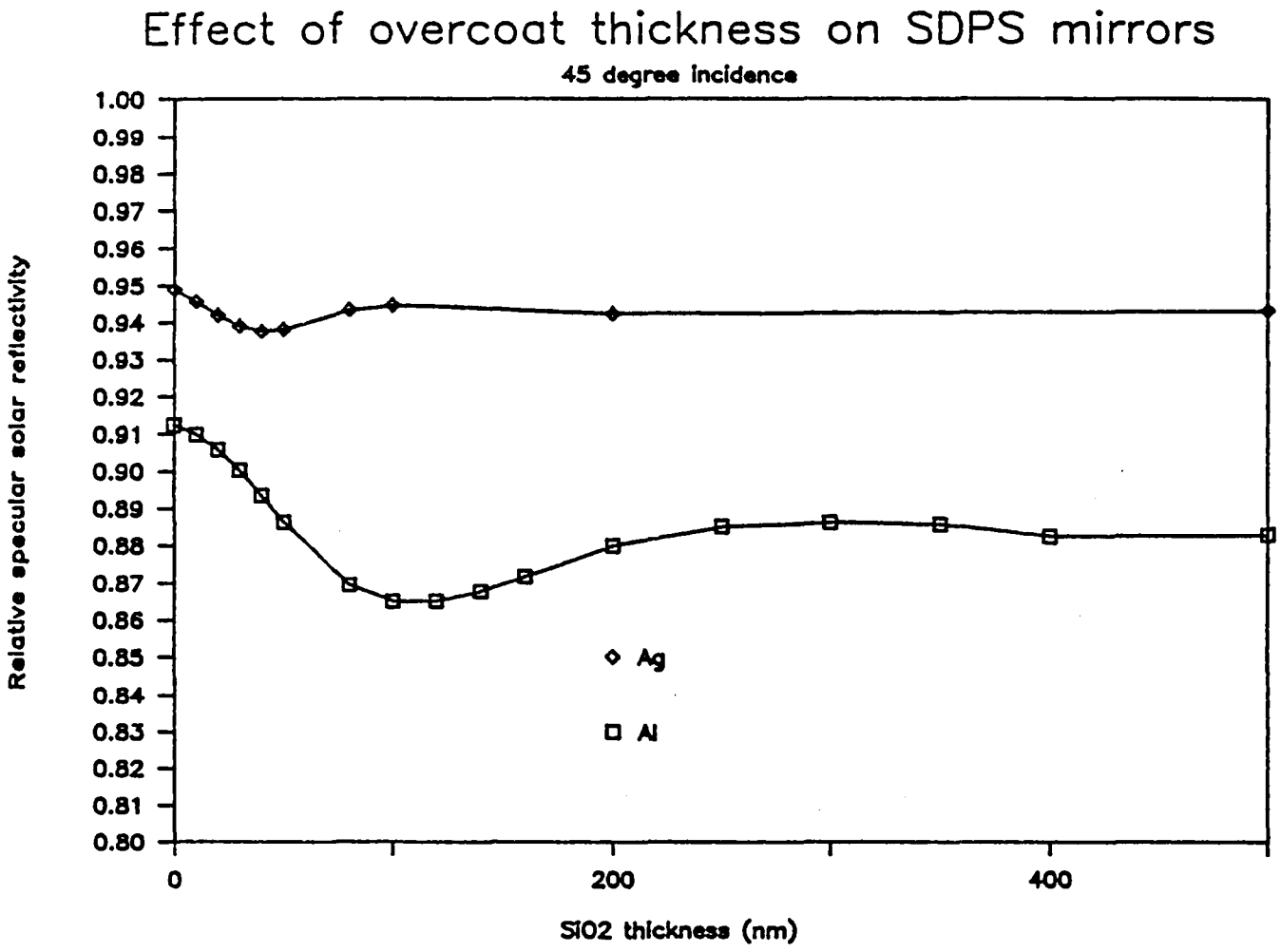

Figure 3-17 Calculated reflectance spectra averaged over AM0 for Ag and Al as a function of SiO_2 overcoat thickness at 45° angle of incidence.

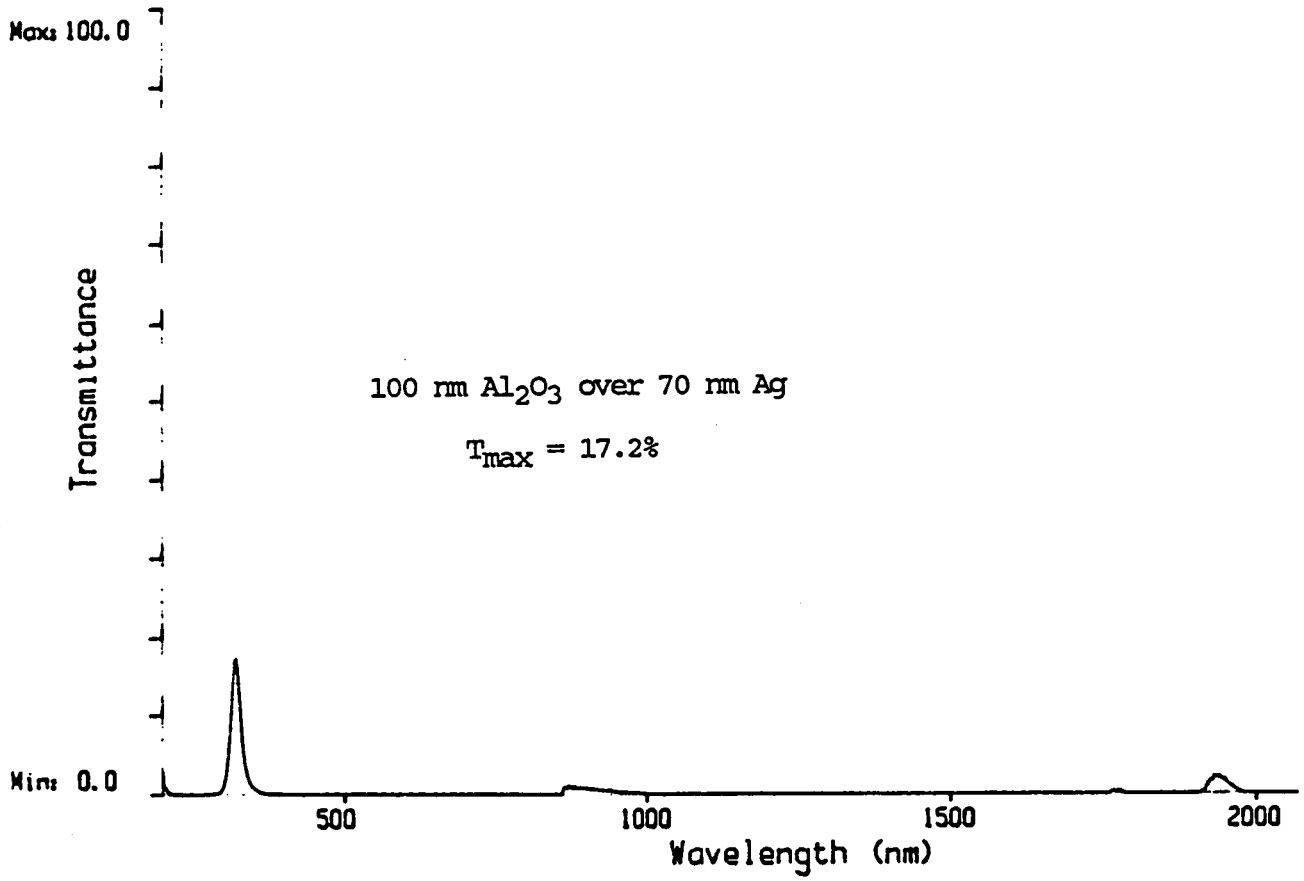

Figure 3-18 Measured transmission spectrum of Ag film.

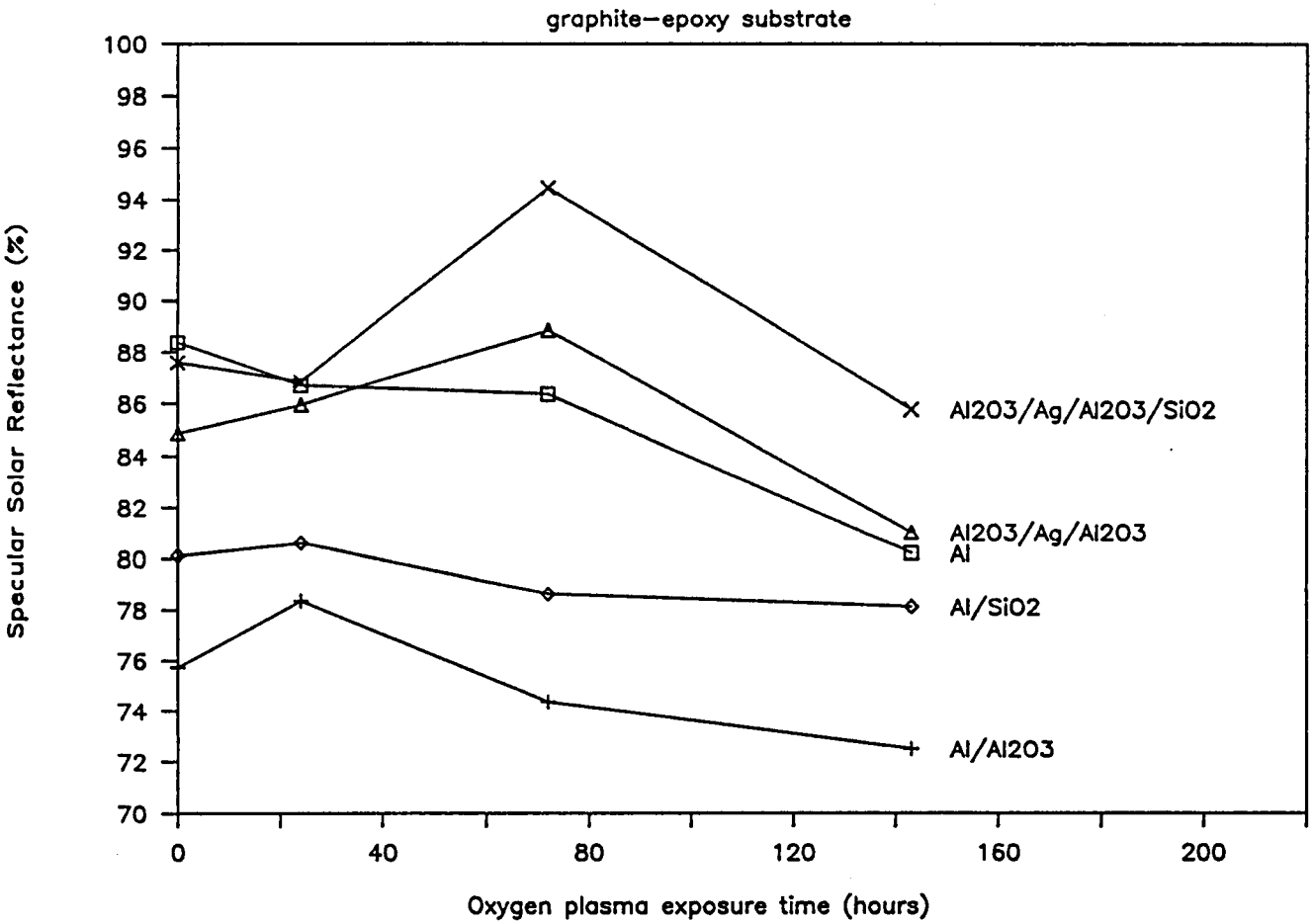

Figure 3-19 Specular reflectance as a function of oxygen plasma exposure time for samples prepared on graphite-epoxy substrates.

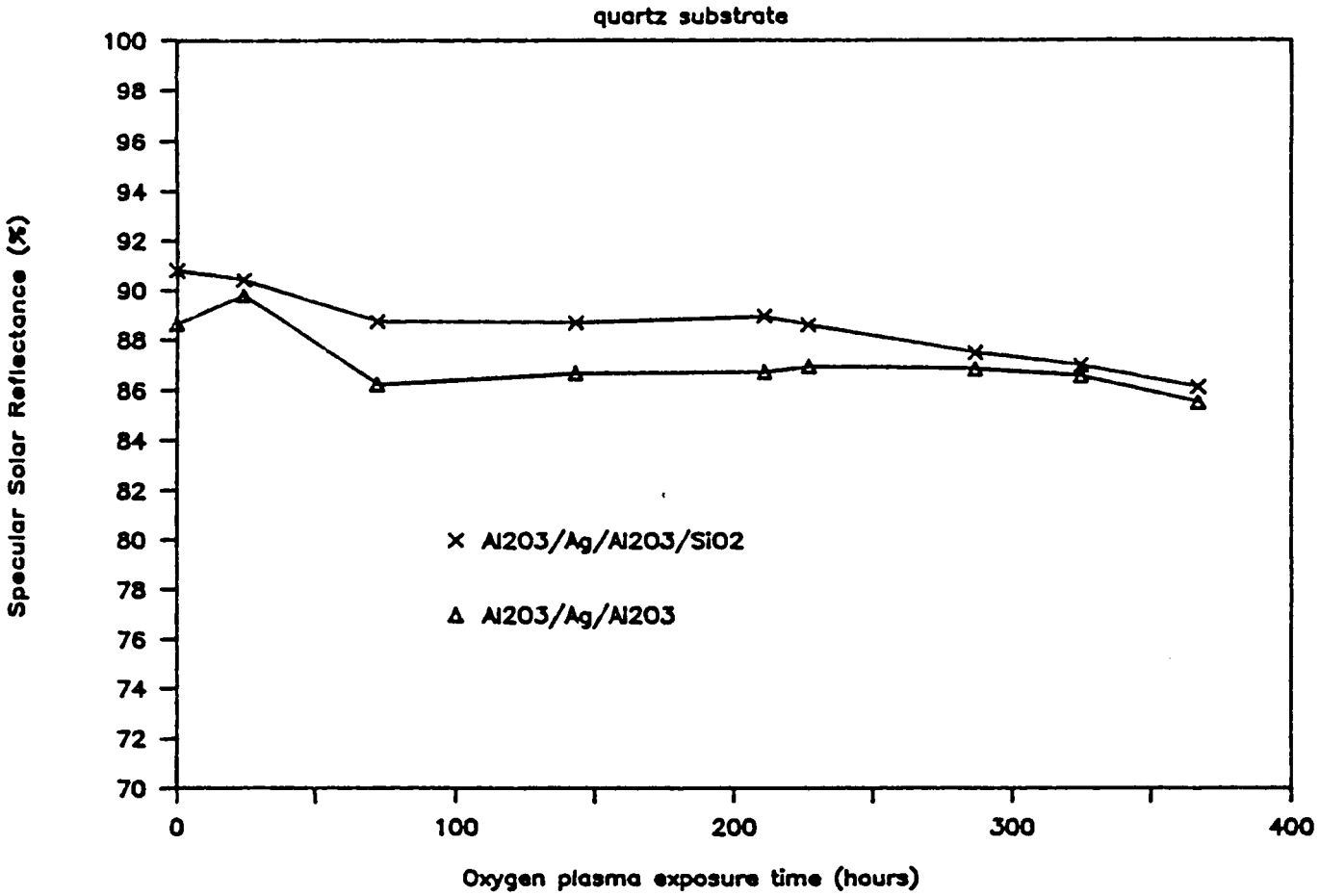

Figure 3-20 Specular reflectance as a function of oxygen plasma exposure time for samples prepared on quartz substrates.

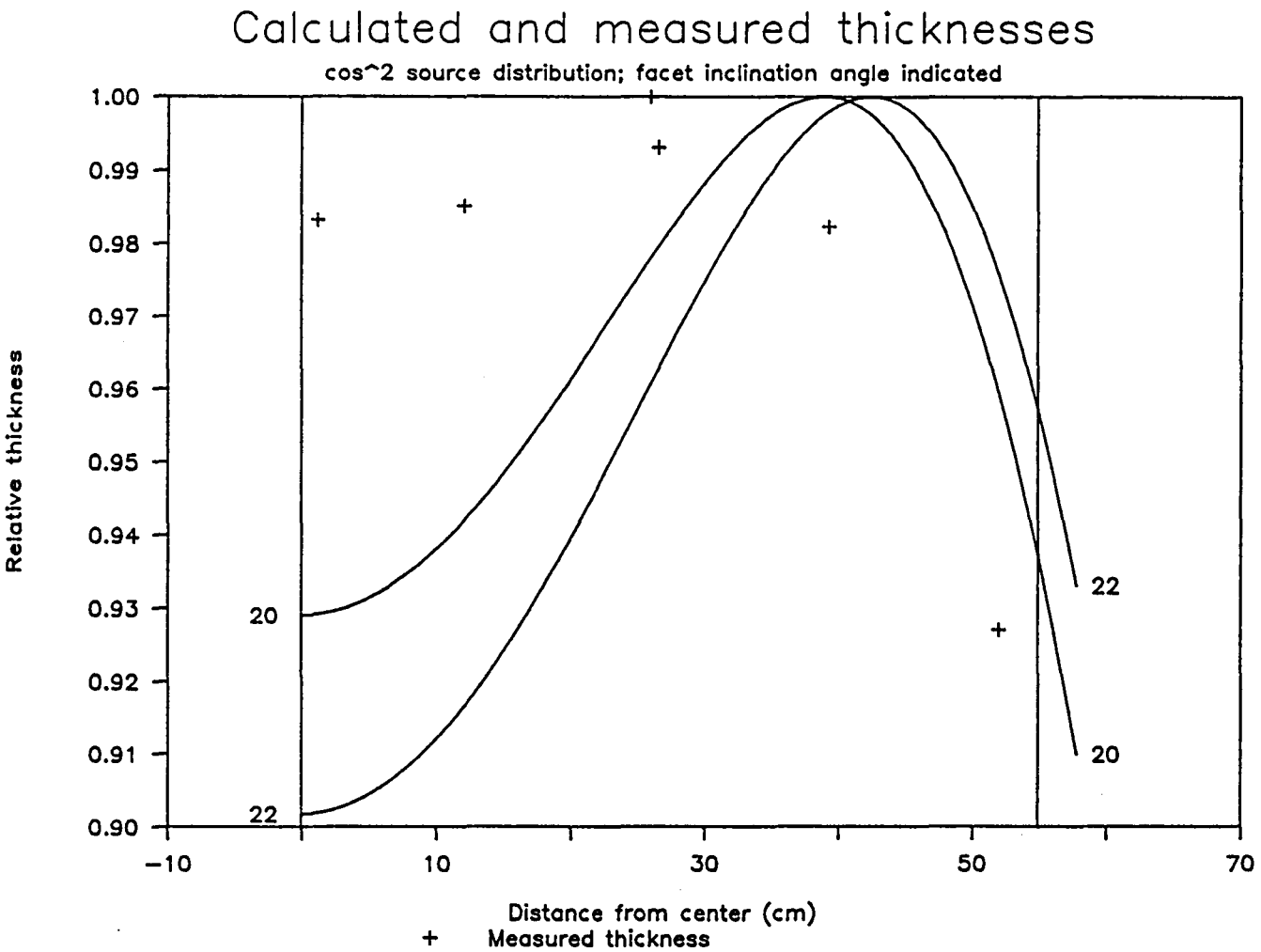

Figure 3-21 Thickness of SiO_2 as a function of position on the facet measured for calibration run.

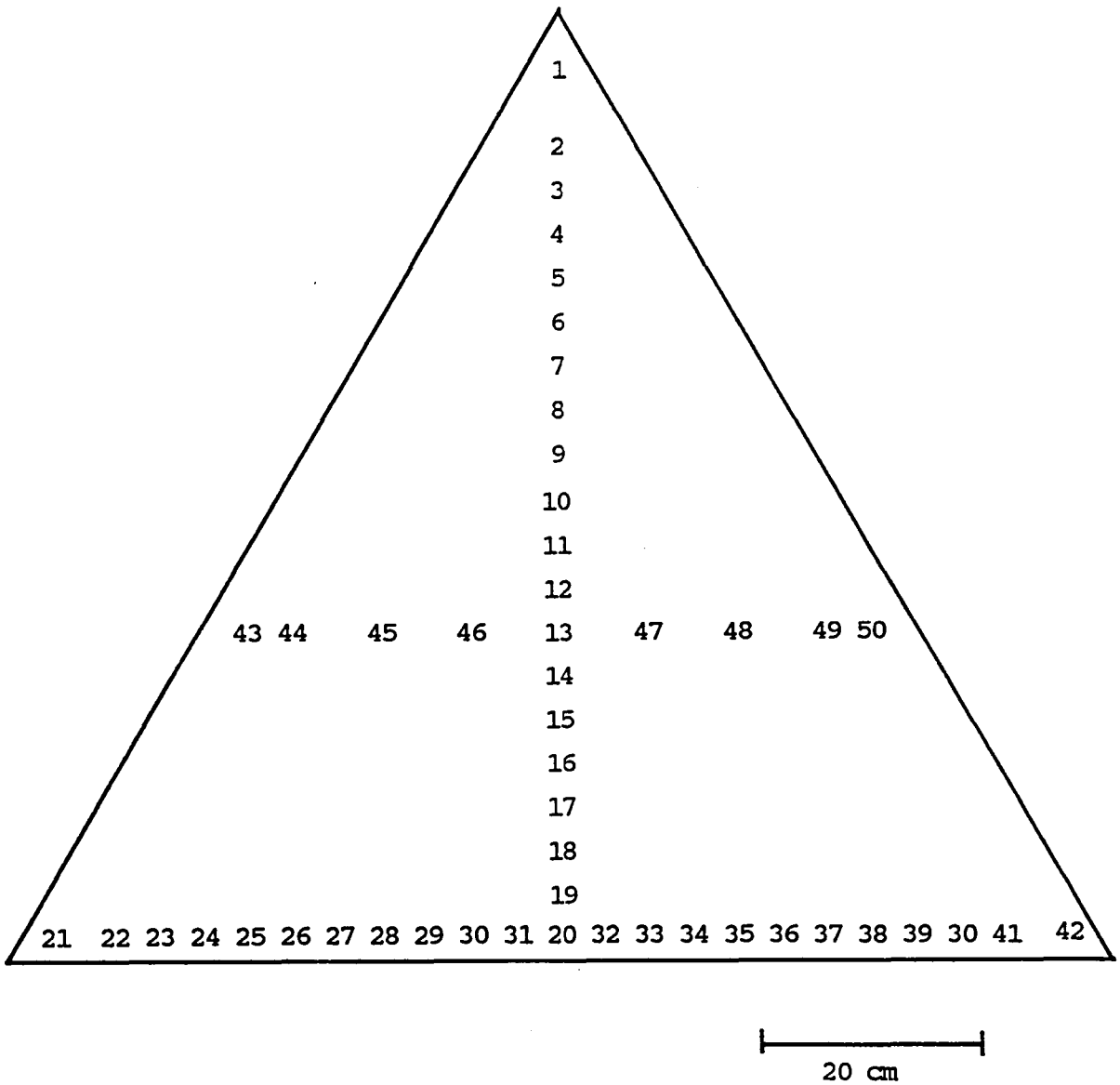

Figure 3-22 Schematic diagram indicated position of coupons on facet mock-up.

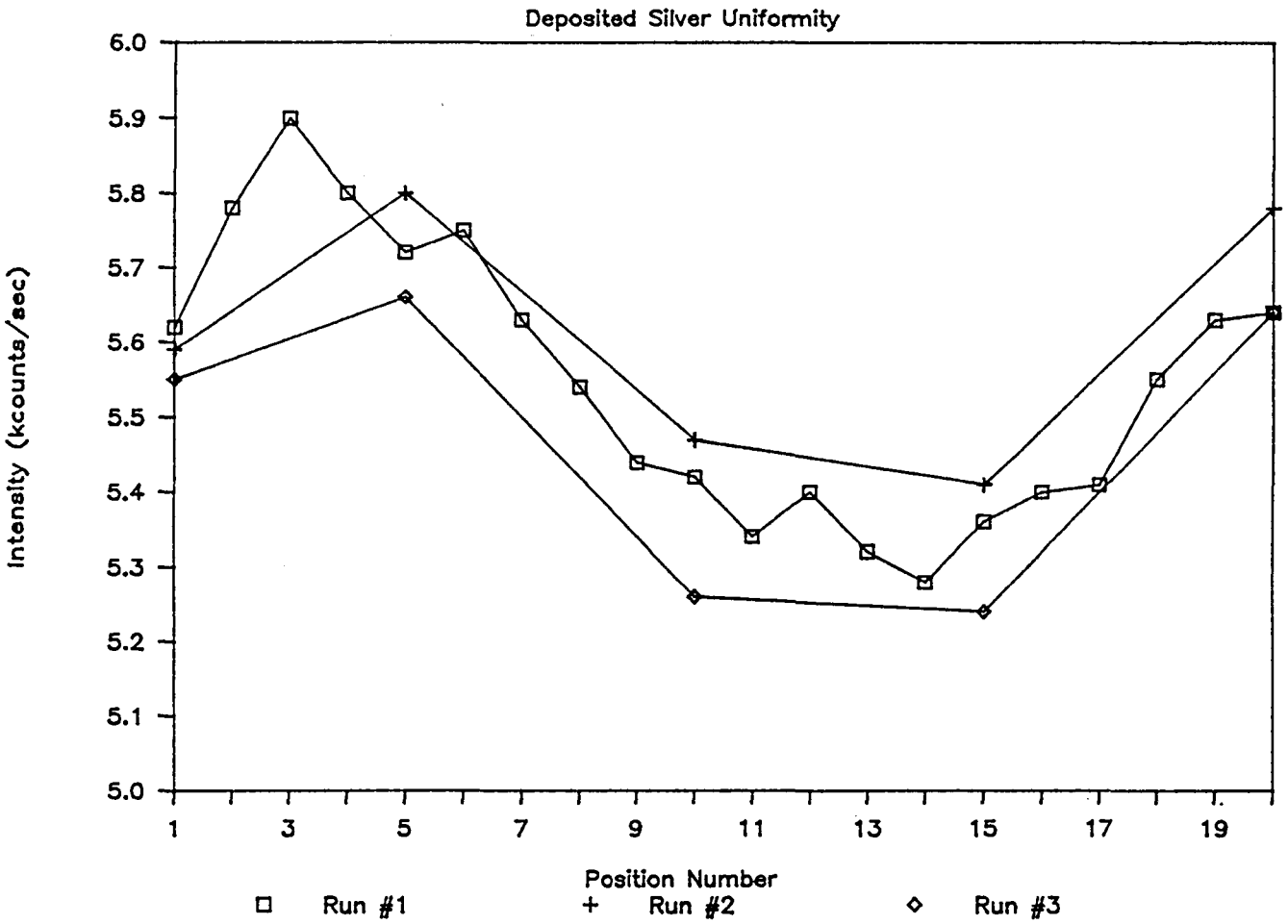

Figure 3-23 X-ray fluorescence data for Ag plotted as a function of coupon number.

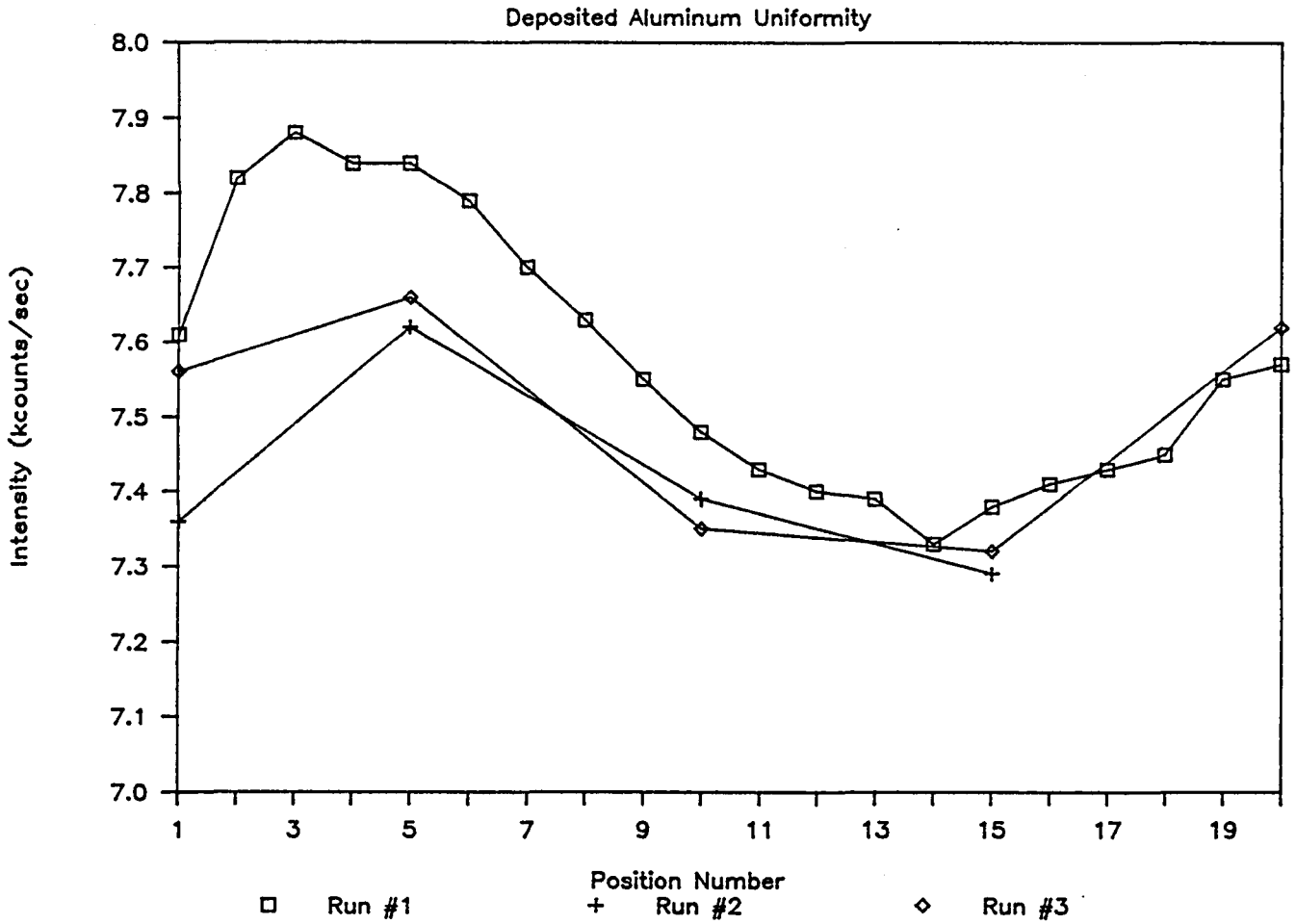

Figure 3-24 X-ray fluorescence data for Al plotted as a function of coupon number.

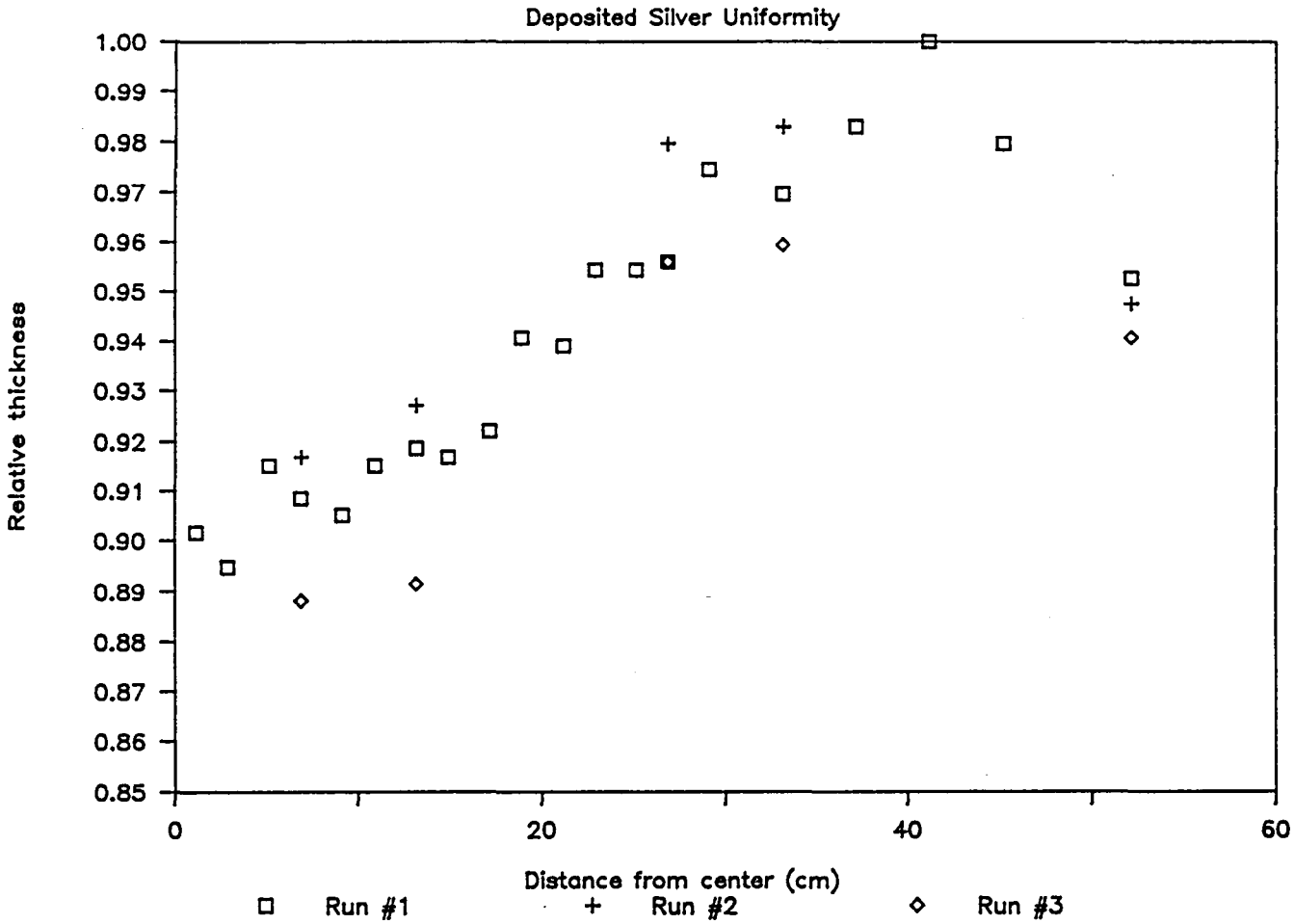

Figure 3-25 X-ray fluorescence data for Ag plotted as a function of distance from the center of the facet.

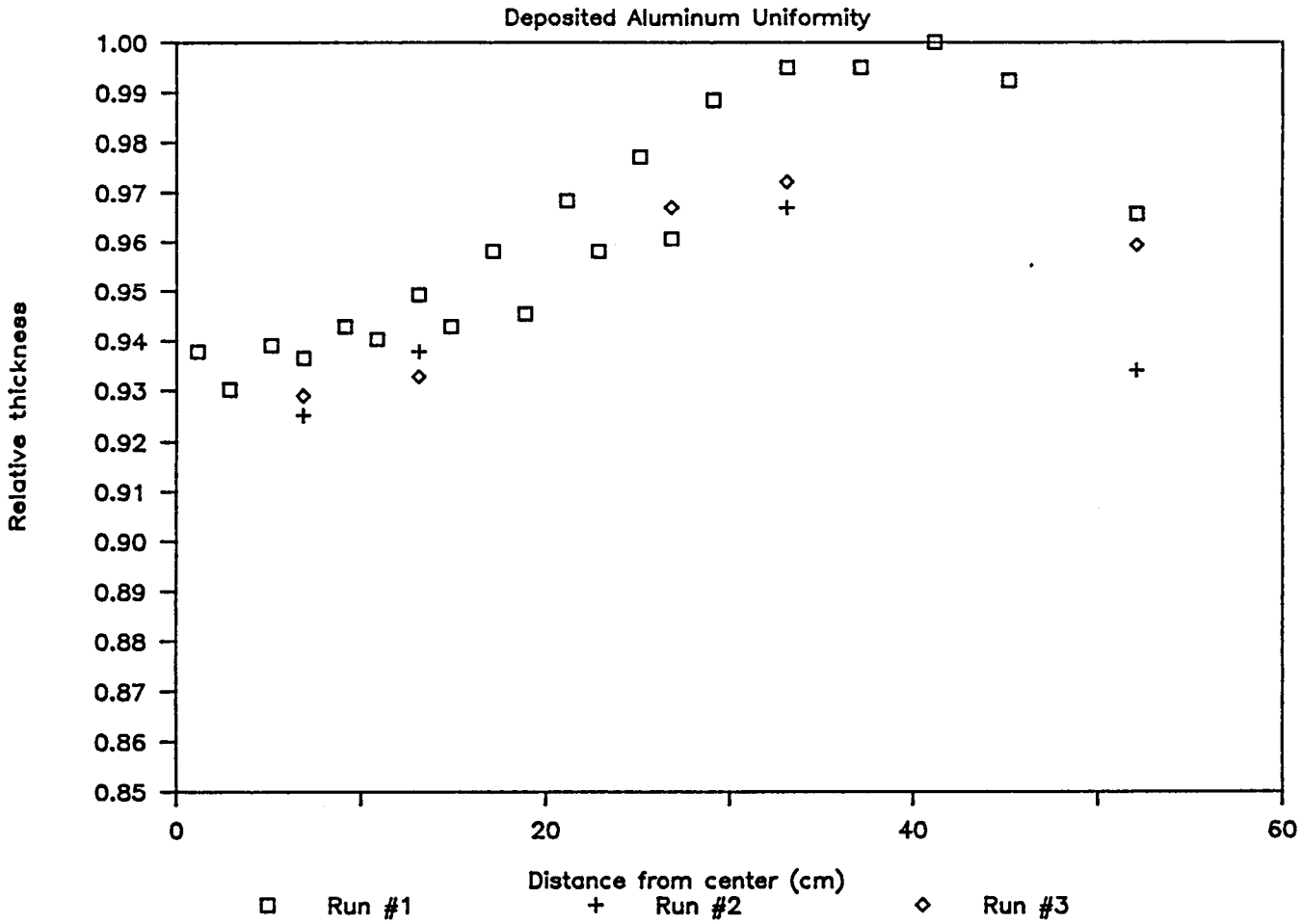

Figure 3-26 X-ray fluorescence data for Al plotted as a function of distance from the center of the facet.

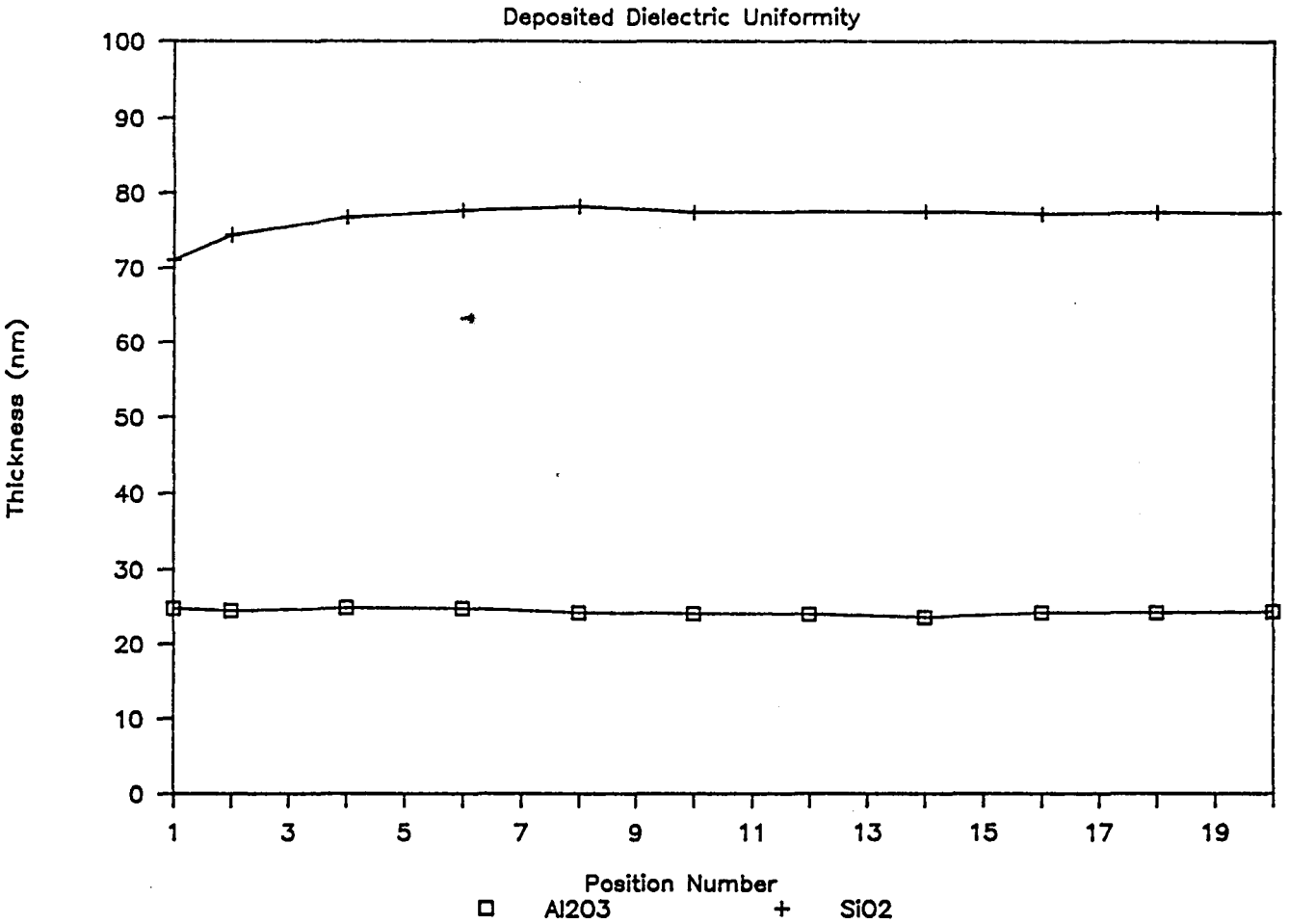

Figure 3-27 Absolute ellipsometric thickness results for Al_2O_3 and SiO_2 plotted as a function of position.

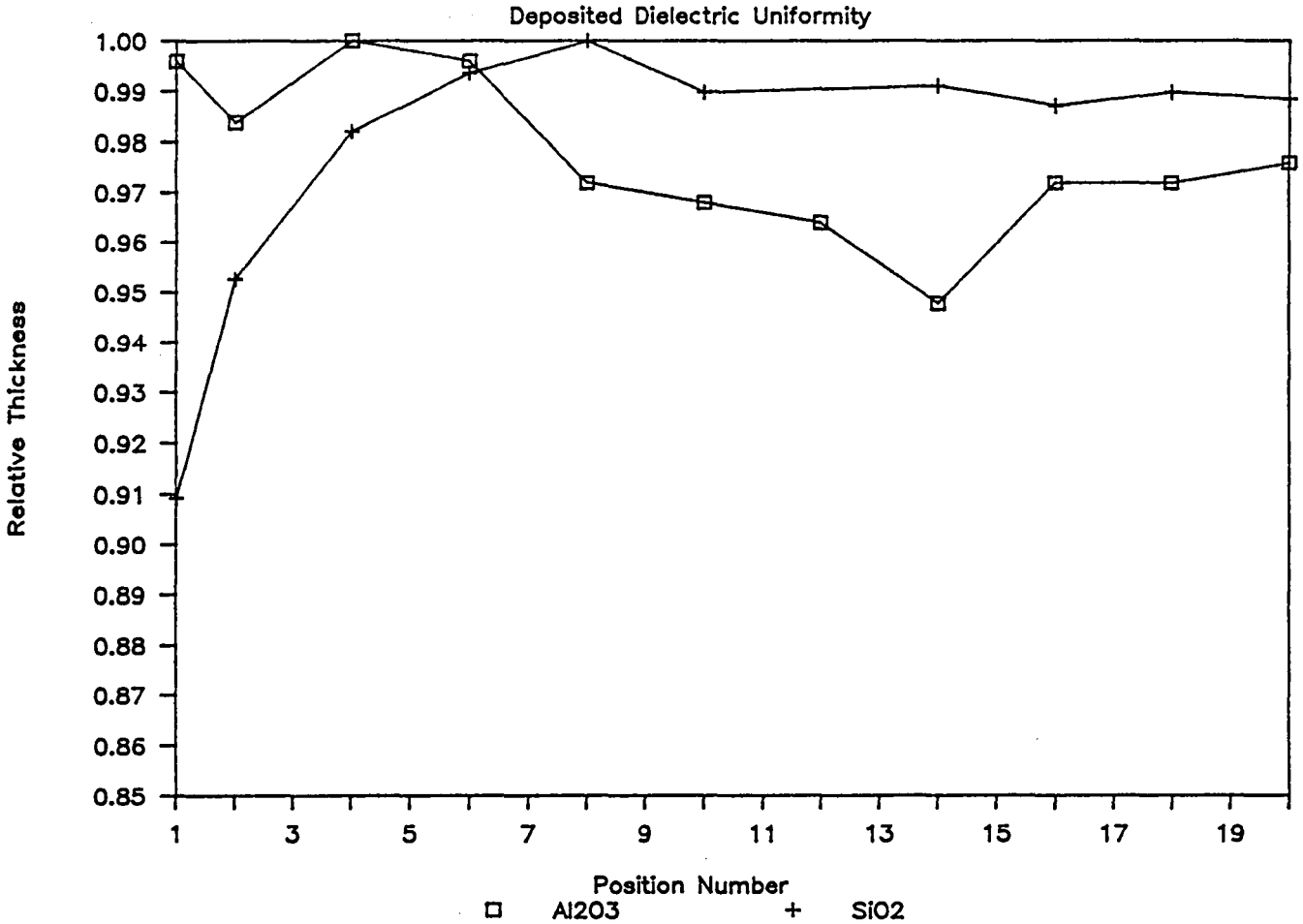

Figure 3-28 Relative ellipsometric thickness results for Al_2O_3 and SiO_2 plotted as a function of position.

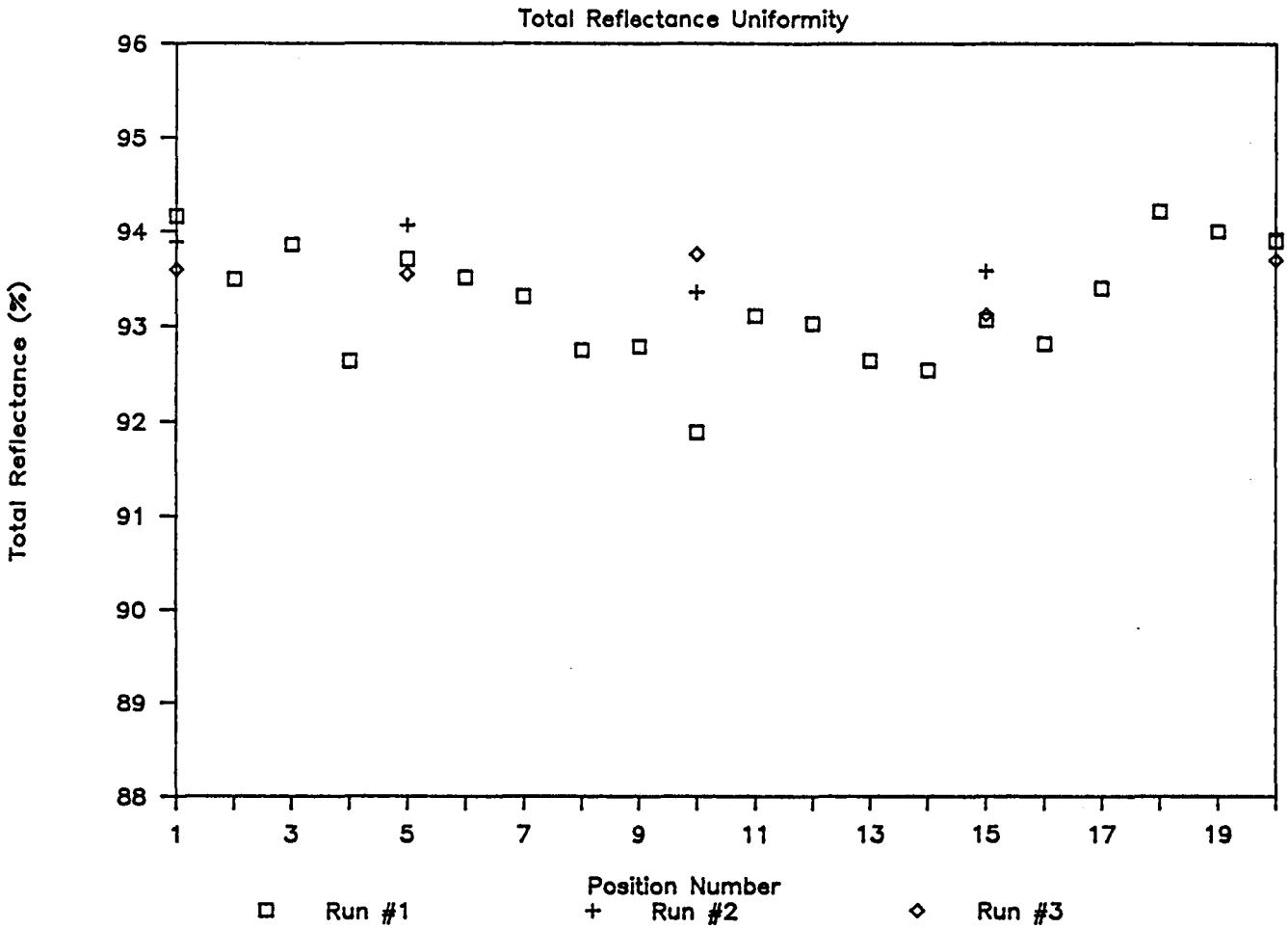

Figure 3-29 Total reflectance uniformity.

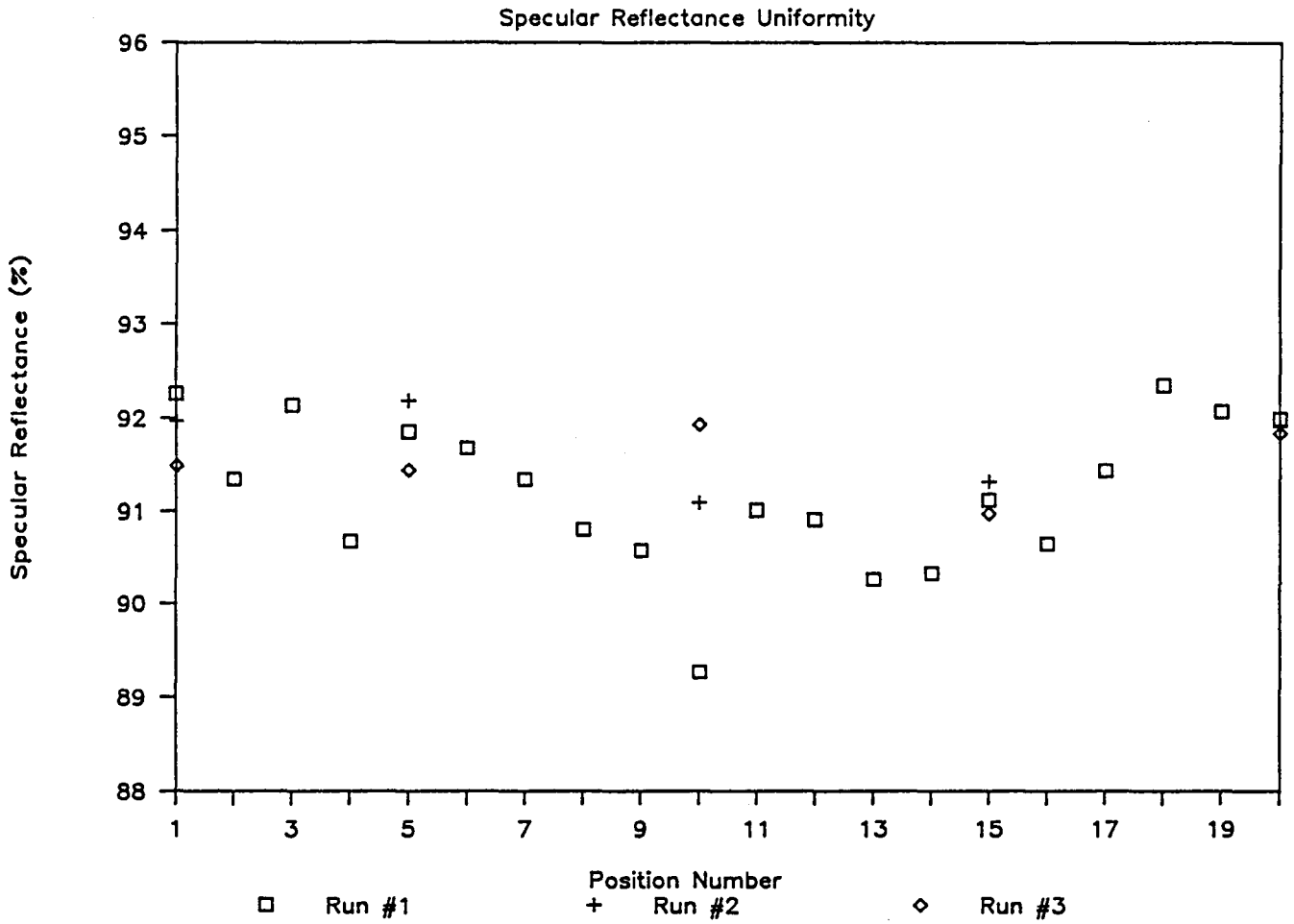

Figure 3-30 Specular reflectance uniformity.

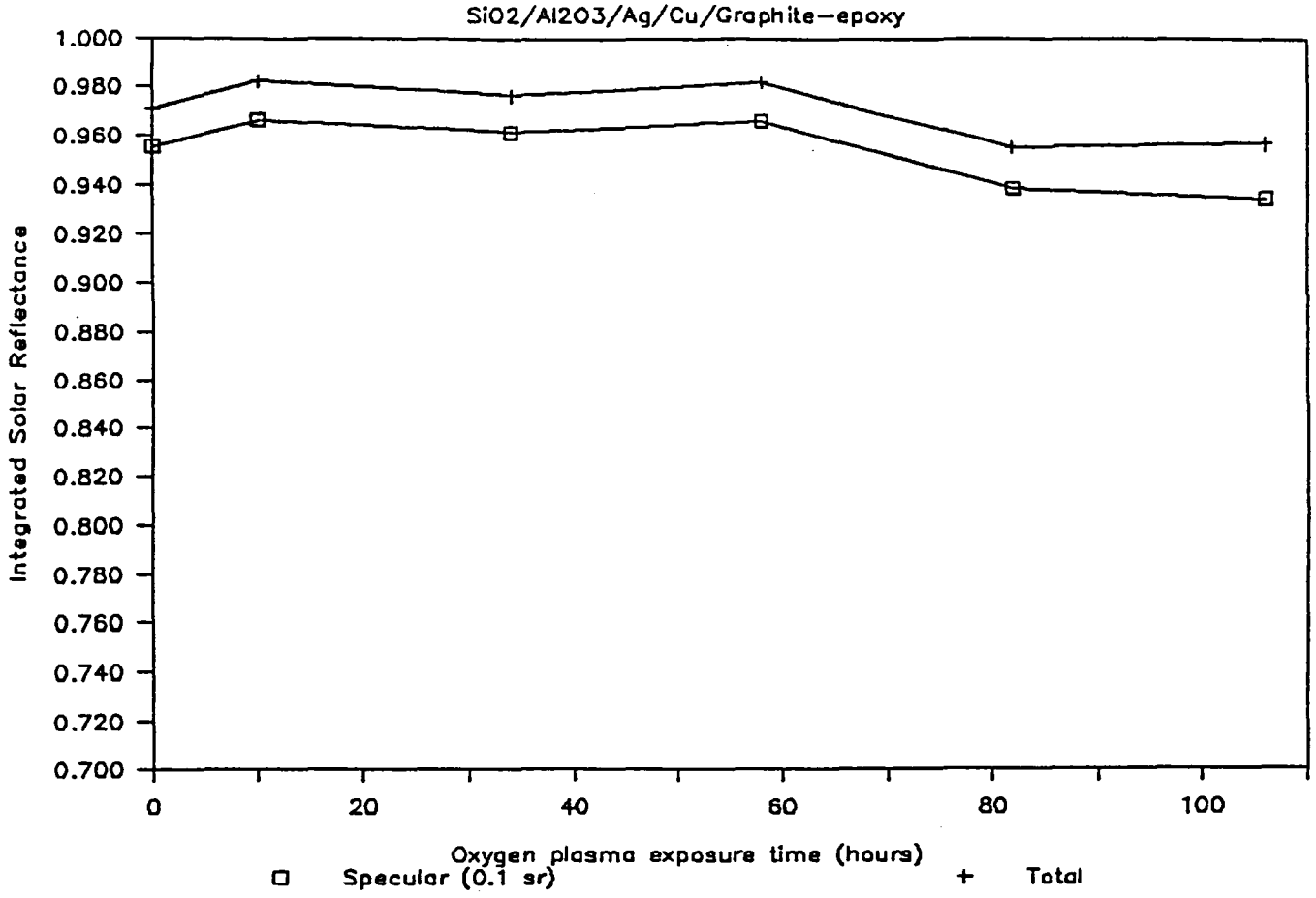

Figure 3-31 Specular reflectance as a function of oxygen plasma exposure time for sample prepared on graphite-epoxy substrate (from D. A. Gulino).

NASA
National Aeronautics and Space Administration

Report Documentation Page

1. Report No.	2. Government Accession No.	3. Recipient's Catalog No.
NASA CR-4158		

4. Title and Subtitle

Design and Demonstration of a System for the Deposition of Atomic-Oxygen Durable Coatings for Reflective Solar Dynamic Power System Concentrators

5. Report Date

July 1988

6. Performing Organization Code

7. Author(s)

Donald J. McClure

8. Performing Organization Report No.

None (E-4150)

10. Work Unit No.

474-52-10

9. Performing Organization Name and Address

3M Corporation
Corporate Research Process Technologies Laboratory
St. Paul, Minnesota 55144

11. Contract or Grant No.

NAS3-25075

13. Type of Report and Period Covered

Contractor Report
Final

12. Sponsoring Agency Name and Address

National Aeronautics and Space Administration
Lewis Research Center
Cleveland, Ohio 44135-3191

14. Sponsoring Agency Code

15. Supplementary Notes

Project Manager, Daniel A. Gulino, Power Technology Division, NASA Lewis Research Center.

16. Abstract

The objectives of this program were to design and demonstrate a system for the vacuum deposition of atomic-oxygen durable coatings for reflective solar dynamic power system (SDPS) concentrators. The design issues pertinent to SDPS were developed by the Government Aerospace Systems Division of the Harris Corporation and are described in NASA CR-179489. Both the design phase and the demonstration phase have been completed. At the time of this report the deposition system was ready for coating of facets for SDPS concentrators. The materials issues relevant to the coating work were not entirely resolved however. These issues can only be resolved when substrates which are comparable to those which will be used in flight hardware are available. The substrates available during the contract period were deficient in the areas of surface roughness and contamination. These issues are discussed more thoroughly in the body of the report.

17. Key Words (Suggested by Author(s))	18. Distribution Statement
Solar dynamic concentrator, Solar mirror, Facet coatings, Solar mirror coatings, Atomic-oxygen durability	Unclassified - Unlimited Subject Category 20

19. Security Classif. (of this report)	20. Security Classif. (of this page)	21. No of pages	22. Price*
Unclassified	Unclassified	68	A04

NASA FORM 1626 OCT 86

*For sale by the National Technical Information Service, Springfield, Virginia 22161

NASA-Langley, 1988

End of Document